CANADIAN JOURNAL OF REMOTE SENSING
2018, VOL. 44, NO. 1, 67–87
https://doi.org/10.1080/07038992.2018.1437719

Taylor & Francis
Taylor & Francis Group

Disturbance-Informed Annual Land Cover Classification Maps of Canada's Forested Ecosystems for a 29-Year Landsat Time Series

Txomin Hermosilla [a], Michael A. Wulder [b], Joanne C. White [b], Nicholas C. Coops [a], and Geordie W. Hobart[b]

[a]Integrated Remote Sensing Studio, Department of Forest Resources Management, University of British Columbia, 2424 Main Mall, Vancouver, BC, V6 T 1Z4, Canada; [b]Canadian Forest Service (Pacific Forestry Centre), Natural Resources Canada, 506 West Burnside Road, Victoria, British Columbia, V8Z 1M5, Canada

ABSTRACT

Land cover classification of large geographic areas over multiple decades at an annual time step is now possible based upon free and open access to the Landsat data archive. Annual gap-free, best-available-pixel, surface reflectance, image composites and annual forest change maps have been generated for Canada for the years 1984 to 2012. Using these data, we demonstrate the Virtual Land Cover Engine (VLCE), a framework for change-informed annual land cover mapping, over the 650 million ha forested ecosystems of Canada, to produce a 29-year data cube of land cover. Post-processing aimed to reduce spurious class transitions is undertaken integrating change information, land cover transition likelihoods, and year-on-year class membership likelihoods. Validation was assessed for a single year (2005) using independent data for an overall accuracy of 70.3% (± 2.5%). Key results are the detailed capture of trends in land cover, illustration of land cover links to disturbance processes, and insights related to the general stability of land cover over time with stand replacing disturbance followed by regeneration of forests. The portable mapping framework and resultant data products offer an integrated, long baseline, disturbance-informed and detailed depiction of land cover to meet science and program related information needs.

ARTICLE HISTORY
Received 10 December 2017
Accepted 2 February 2018

1. Introduction

Land cover is a biophysical indicator that refers to both the observed biotic and abiotic assemblage of Earth's surface, including the vegetation and anthropogenic structures covering the land (Hansen and Loveland 2012; Meyer and Turner 1992). Changes in land cover have a strong influence on hydrology, climate, and global biophysical and biogeochemical cycles of the terrestrial surface, occurring at a range of spatial scales and at a variety of temporal rates (Pielke et al. 2011; Skole et al. 1997). Mapping land cover and quantifying related changes in physical characteristics is critical to understand and monitor the status and conditions of ecosystems (Henderson-Sellers and Pitman 1992). Both land cover and land cover change are key information needs when monitoring terrestrial ecosystems, informing on status and trends for reporting, as well as providing critical model inputs for carbon budgets, habitat, biodiversity, and resource management activities.

Remote sensing has emerged as a mature technology for mapping land cover across a range of spatial scales. Many nations have established operational land cover mapping and monitoring programs using moderate resolution satellite data in order to fulfill key information needs related to science, policy, and management, e.g., CORINE (Bossard et al. 2000); NLCD (Homer et al. 2004); EOSD (Wulder et al. 2008). These programs rely on remotely sensed data to produce detailed, temporally updated, spatially explicit, maps of land cover (Foody 2002). Land cover is typically mapped using signature-extension methods, which involve portable signatures from known geographic locations (i.e., training sample units) to extrapolate the relationship at the known pixel to the unknown, located at specific distances in time and space (Olthof et al. 2005; Woodcock et al. 2001).

The opening of the United States Geological Survey (USGS) archive of Landsat imagery (Woodcock et al. 2008) has provided free access to high-quality geometrically and spectrally analysis-ready imagery at spatial and temporal resolutions that are appropriate to depict both natural and anthropogenic land cover changes in terres-

CONTACT Txomin Hermosilla txomin.hermosilla@ubc.ca; txominhermos@gmail.com Integrated Remote Sensing Studio, Department of Forest Resources Management, University of British Columbia, 2424 Main Mall, Vancouver, BC, V6T 1Z4, Canada.
Color versions of one or more of the figures in the article can be found online at www.tandfonline.com/ujrs.

trial ecosystems (Wulder and Coops 2014; Wulder et al. 2012). This has facilitated an increased focus on mapping of large areas, from regional to global scales (Griffiths et al. 2013; Roy et al. 2015; White et al. 2014), as well as novel robust time-series approaches focused on spectral-trend analysis to detect, describe, and identify changes in vegetation and vegetation condition (Hermosilla et al. 2015a; Huang et al. 2010; Kennedy et al. 2010; Schroeder et al. 2017; Verbesselt et al. 2010; Zhu and Woodcock 2014). Azzari and Lobell (2017) link the increase in computing capacity for storage and analysis (i.e., cloud-based platforms) with opportunities for increasingly customized and application-specific land cover maps. A remaining challenge for development of new methods for mapping of land cover and land cover change over space and time is the meaningful integration of the temporal dimension and the incorporation of logical class transitions as well as knowledge of succession and disturbance processes (Gómez et al. 2016).

The expectation underpinning classification algorithms is that Landsat's surface reflectance values will be the same for features presenting the same physical characteristics (Hansen and Loveland 2012). This understanding can also be extended across time, allowing for an expectation that the same features at a different time will have the same reflectance characteristics. At a given location, the reflectance can be expected to change due to disturbance or successional processes, or remain largely the same, such as for non-vegetated features. The consistency of surface reflectance values over space and time supports the application of statistically driven mapping approaches. This implies that spectral conditions for a specific class at a given location can be mapped to that class with similar spectral conditions elsewhere—over both space and time (Song et al. 2001).

Though not recommended, land cover change detection has often been addressed via thematic or post-classification comparisons (for cautions against see Fuller et al. 2003), where any error or uncertainty present in either of the individual date land cover classifications will be multiplied and propagated in the final land cover change map (Coppin et al. 2004; Fuller et al. 2003). Spectral time-series analysis approaches can provide metrics to describe land cover change and vegetation dynamics to assist in the generation of multiple, integrated, sequential, land cover products, which—when combined with knowledge of ecological succession—can support temporally consistent land cover mapping (Gómez et al. 2016). Land cover and land cover change have typically been estimated separately and not necessarily integrated, especially for projects over large areas. Integrating land cover and land cover change allows for the development of algorithms that are temporally informed and that control for change. Knowledge of a given category (and associated class likelihoods) through time allows for quantitative refinement of spectrally estimated land cover classes for a multi-decadal temporal stack of images (Abercrombie and Friedl 2016). Knowledge of where, when, and what land cover changes have occurred allow for algorithm developments that improve class allocations, class transitions, and the incorporation of class transition logic and successional expectations (Cai et al. 2014). Forest ecosystems comprise many features that are largely invariant, such as water bodies. Conversely, there are other landscape features not subject to disturbance that retain a given land class over time yet vary qualitatively within that category, such as a maturing forest of a given cover type. Fire and harvesting activities result in a change in land cover, but also in expected trajectories of development or succession through a given set of land cover classes (Bergeron and Harvey 1997). The thematic land cover products generated with this framework provide valuable information on land cover dynamics and changes, which are required to meet national science, monitoring, and reporting information needs, as described in White et al. (2014).

Annual land cover maps are useful for supporting a broad range of science, monitoring, and reporting objectives. Automated methods that use Landsat time series to estimate annual land cover products over large areas are nascent (Gómez et al. 2016). In this paper, we present an automated framework to integrate change information estimated from the analysis of Landsat time series with knowledge of ecological succession to produce a temporally consistent annual series of land cover maps for Canada's forested ecosystems for the period 1984 to 2012. The Virtual Land Cover Engine (VLCE) framework is based upon the efficient and transparent generation of land cover and allows for flexibility of inputs such as calibration data that are representative of a given land cover legend. Herein, we describe each component of the methodological framework, including data inputs, training data, classification algorithm, and data-driven post-classification refinements. We also report the results of an independent national accuracy assessment of the land cover products generated, and characterize land cover dynamics of Canada's forested ecosystems from 1984 to 2012. The VLCE is an integrated workflow that enables change-informed land cover to be generated on an annual time step, underpinned by best-available pixel surface reflectance image composites, change information, a target land cover legend, knowledge of ecological transitions between target classes, and suitable training data for model development. Due to the open access nature of the Landsat archive, the VLCE framework presented is portable and can be adapted to specific information needs of differing user communities (e.g., classification schema) and is also flexible to differing training data sources.

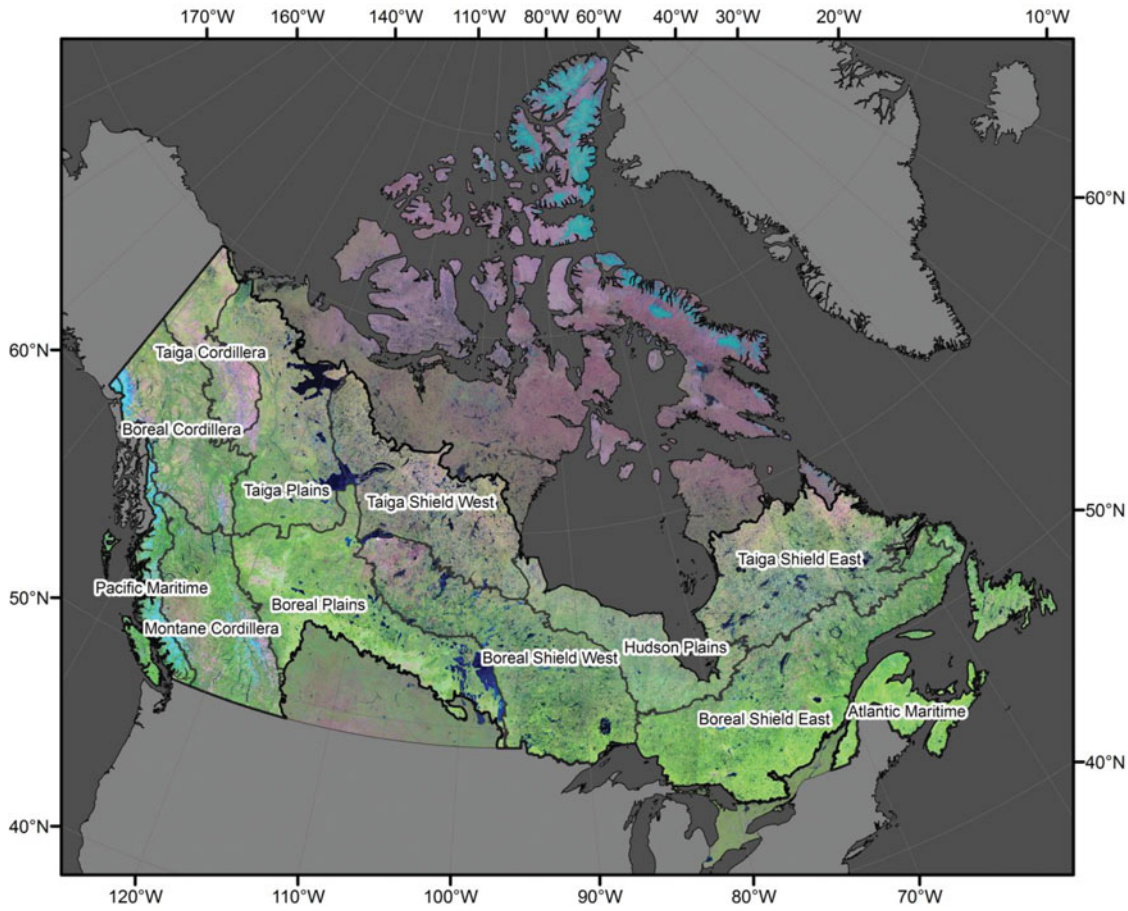

Figure 1. False color (bands: SWIR, NIR, R) Landsat best-available-pixel (BAP) composite of Canada in 2010 overlaid with Canada's forest-dominated ecozones.

1.1. Study area

Canada is 998.5 million hectares in area, with forested ecosystems occupying ~650 million ha, or 65% of the national area (Wulder et al. 2008). The forest-dominated ecosystems are identified following the ecozone stratification of Canada (Ecological Stratification Working Group 1995) shown in Figure 1. These forest-dominated ecozones are mainly a mixture of trees, shrubs, wetlands, and lakes (Wulder et al. 2008). Within the forested ecosystems, Canada's National Forest Inventory reports that forests (treed and other wooded land) in Canada occupy 347.1 million ha (National Resources Canada 2016).

2. Methods

In this research, we present the VLCE: an automated framework to enable annual land cover mapping using a time series of Landsat surface reflectance, and informed by spatially explicit forest change and *a priori* knowledge of ecological succession. The VLCE framework, summarized here and detailed below, is transferable and flexible, so users can adapt the desired land cover legend based upon their training data availability and intended use of maps produced. Figure 2 shows the conceptual workflow of the annual land cover classification framework proposed. We used the Canada-wide seamless surface-reflectance composites and time-series forest change information products from 1984 to 2012 generated with the Composite-2-Change (C2C) approach presented in Hermosilla et al. (2016). To offer additional classification discrimination, we utilized elevation information derived from the ASTER Global Digital Elevation Map (GDEM) product. Based on the Earth Observation for Sustainable Development of forests (EOSD) land cover product classes, initial annual land cover classifications were generated by extending the training signatures to the surface reflectance values from each year using Random Forests classifier. Based upon the class probabilities provided by Random Forests votes, the post-classification process was informed by forest change and ecological succession. This post-processing step comprises the application of a Hidden Markov Model to stabilize land cover transition predictions through time in order to produce temporally consistent land cover maps, as well as the application of logical land cover transition rules to restrict unlikely land cover transition predictions. We assessed the land

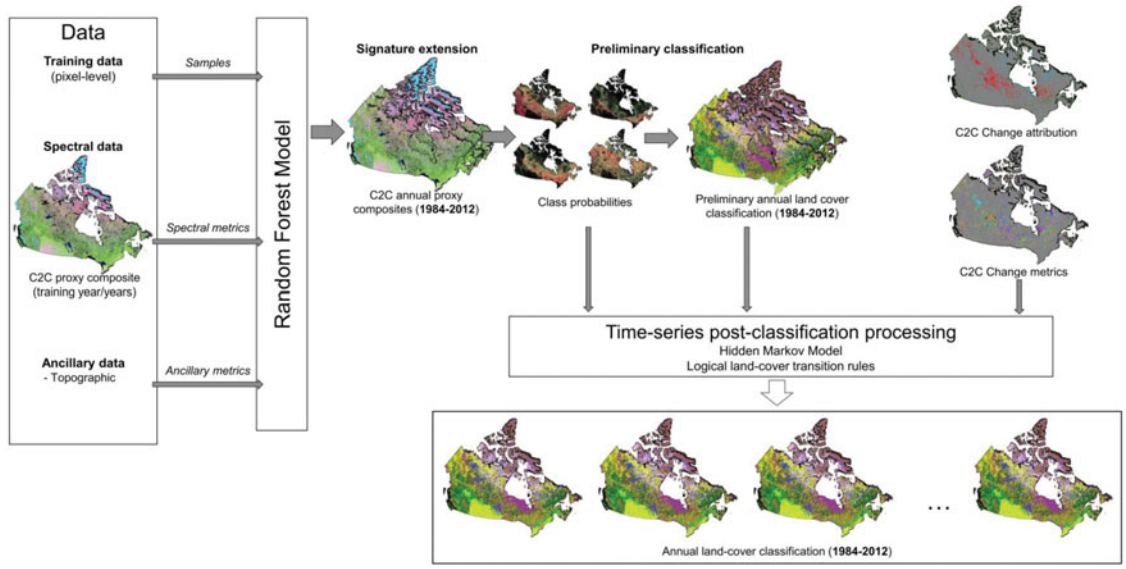

Figure 2. Conceptual workflow of the Virtual Land Cover Engine (VLCE) framework for producing annual land cover classifications using the image composites and forest change information produced using the Composite-2-Change (C2C) approach (Hermosilla et al. 2016).

cover classification accuracy with an independent set of validation sample units, and enumerated on the particulars of land cover transitions before and after the post-classification step. While the VLCE theoretically enables national mapping of Canada's land cover, our special focus is on the forested ecosystems, hence we reported and analyzed land cover and land cover changes in Canadian's forest-dominated ecosystems from 1984 to 2012, characterizing land cover dynamics following wildfire and harvesting events.

2.1. Data

2.1.1. Landsat time-series data and derived forest change information

Data inputs included a time series of Landsat derived best-available pixel (BAP) image composites (1984–2012) and forest change information estimated using the C2C approach (Hermosilla et al. 2016). In brief, the C2C approach involves the generation of annual BAP image composites by choosing the optimal observations for each pixel from all available archived Landsat-5 TM and -7 ETM+ imagery. The input Landsat images are atmospherically corrected using LEDAPS (Masek et al. 2006; Schmidt et al. 2013) to convert their digital numbers into surface reflectance values using LEDAPS algorithm. *Best* pixels are determined based on the scoring functions defined by White et al. (2014), including proximity to mid-summer target date (Julian day 213 ± 30 days), presence and distance to clouds and their shadows (detected using Fmask algorithm, Zhu and Woodcock 2012), atmospheric quality, and acquisition sensor (priority to Landsat-5 TM over -7 ETM+ after scan line corrector failure in 2003). Once the annual composites are generated, they are further refined to remove noisy observations (unscreened clouds and haze) and to infill data gaps with synthetic values by applying spectral trend analysis to each pixel time series (Hermosilla et al. 2015a). Following this temporal refinement step, the outcome is the production of seamless annual surface reflectance composites (proxy BAP composites; hereafter BAP composites) for all of Canada from 1984 to 2012, as well as the detection and characterization of forest change events. Finally, following the object-based image analysis approach presented in Hermosilla et al. (2015b), forest change was attributed to a change type (i.e., fire, harvest, road, or non-stand-replacing), based on the spectral, temporal, and geometrical characteristics of the change objects. Validation of the attributed change using independent data derived via manual interpretation indicated an overall accuracy of 92% (Hermosilla et al. 2016).

2.1.2. EOSD land cover map

The Earth Observation for Sustainable Development initiative produced a c. 2000 land cover map of the forested ecosystems of Canada (Wulder et al. 2008). The EOSD map was produced using an unsupervised hyperclustering approach, followed by cluster merging and labeling (Wulder et al. 2004). The EOSD land cover map is composed of 23 land cover classes in a hierarchical classification structure following that of the National Forest Inventory (NFI). For this project, we identified 12 target classes from the EOSD/NFI hierarchy for annual mapping (Figure 3). Based upon a regional study, the map accuracy was found to be 77% at the vegetation level (Figure 3), (Wulder et al. 2007).

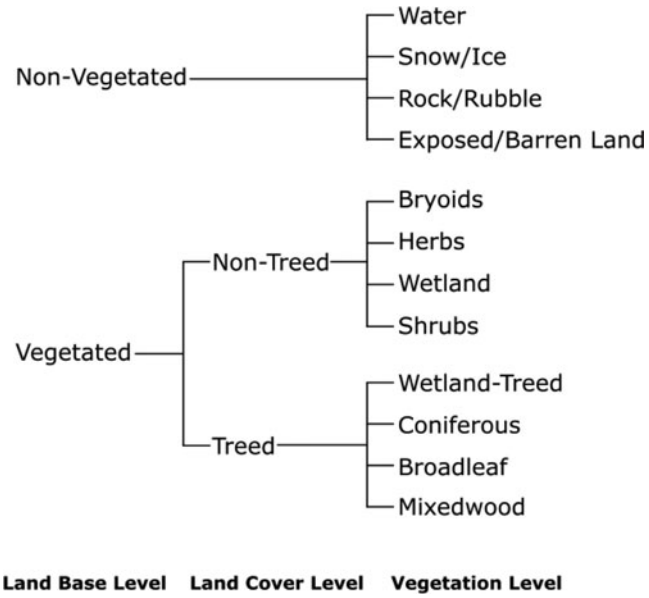

Figure 3. EOSD land cover hierarchy and the 12 classes mapped in this study.

2.1.3. ASTER global digital elevation map

Topographic variables are known to be important predictors for land cover mapping (Wulder et al. 2004). Knowledge of landscape position (elevation) or exposure (aspect) combined with spectral data provides additional information to partition between spectrally similar yet physically different land cover types or vegetation communities (Franklin 1995; Strahler et al. 1978). Version 2 of the ASTER Global Digital Elevation Map was employed to derive topographic variables for use as predictors in our classification approach (Tachikawa et al. 2011). The first version of the ASTER GDEM was released in June 2009 and was generated using stereo-pair images collected by the ASTER instrument onboard the Terra satellite. The improved GDEM v2 included 260,000 additional stereo-pairs, which enhanced the coverage of the product and reduced the occurrence of artifacts. The refined production algorithm improved the spatial resolution of the product (~ 30 m), and increased horizontal and vertical accuracy. GDEM was used to calculate slope (in degrees), and the Topographic Solar Radiation Aspect (TRASP) index after Roberts and Cooper (1989).

2.1.4. Summary of data inputs and outputs

For processing purposes, Canada was partitioned in 41 processing tiles, as result of dividing the country longitudinally–corresponding to the UTM zones from 7 to 22—and latitudinally—South (southern border, 60° N), North (60–70° N), and Arctic (70–83° N) – (Hermosilla et al. 2016). Forested ecosystems resulted in a spatial tessellation of over 7 billion 30-m pixels. The input layers comprised >17 Tb for 29 years of spectral data and spectral indices, topographic variables, and forest change layers. The output layers required 6.7 Tb of storage and included initial classification, votes per class, and post-processed land cover classification layers for the 29 years analyzed (Table 1). To generate a time series of land cover representing 29 years, the VLCE framework used the input layers to generate interim outcomes and final classifications, resulting in the processing of over a trillion pixels.

Table 1. Summary of data inputs and outputs. Section 3.3. lists the spectral indices used as input layers.

Dataset		Data type	Bands	Years	Size (TB)
Input layers	Spectral bands	integer	6	29	5.76
	Spectral indices	float	6	29	11.52
	DEM	integer	1	1	0.03
	Slope and aspect	float	2	1	0.13
	Change year	integer	2	1	0.03
	Change type	byte	1	1	0.02
Result layers	Initial classification	byte	1	29	0.48
	Random Forests votes	byte	12	29	5.76
	Final classification	byte	1	29	0.48
Total					**24.21**

2.2. Training data selection

Training data are a key component for signature generation in supervised land cover classification approaches. Training data collection, however, is difficult in large jurisdictions and over remote areas (Inglada et al. 2017). Moreover, access to spatio-temporally consistent historical data with suitable information, classes and/or spatial distribution to train multi-temporal land cover classification models is especially challenging. In this research, we build upon Zhu et al. (2016) and generate training signatures using pixels derived from the c. 2000 EOSD land cover map (Section 3.1.2). Note that our validation approach is described below and is based upon purpose-collected and independently interpreted sample units using high spatial resolution satellite data, not on reserved sample units derived from the EOSD. Since land cover products intrinsically include some level of error, precautions were considered to minimize errors in our training data. Thus, we aimed to avoid the use of border pixels, ensuring the sample units were located ≥90 m away from other land cover classes (Pelletier et al. 2016). We selected a large random sample of 300,000 pixels per class, resulting in 3,600,000 training pixels (representing 0.05% of the EOSD land cover map's population). The calibration sample units were distributed proportionally across the spatial extent of Canada's forest ecosystems to enable the capture of each classes' regional particularities.

2.3. Selection of predictors for classification

From the year 2000 BAP composite, we generated a set of potential spectral metrics to use as predictors in our land cover modeling (with the year 2000 BAP corresponding to the EOSD c. 2000 training sample). These predictors included surface reflectance for bands 1–5 and 7, Normalized Vegetation Index (NDVI) (Tucker 1979), Normalized Burn Ratio (NBR) (Key and Benson 2006), Enhanced Vegetation Index (EVI), Automated Water Extraction Index (AWEI) (Feyisa et al. 2014), and Tasselled Cap components including Greenness (TCG), Brightness (TCB) and Wetness (TCW) (Crist 1985). Additionally, we included the topographic metrics generated from the ASTER GDEM: elevation, slope, and TRASP (Section 3.1.3). To avoid any negative impacts on model definition and subsequent classification results (Brosofske et al. 2014), we evaluated the degree of multicollinearity among the candidate predictors and removed those having a Pearson's $R > 0.80$. This reduced the number of candidate predictors from 16 to 7. The final set of inputs therefore included surface-reflectance values of bands 4 and 7, EVI, TCG, elevation, slope, and TRASP. Values for these 7 predictors were extracted for each of the training pixel locations for development of the land cover model.

2.4. Classification algorithm and preliminary annual land cover classification

A Random Forests classifier (Breiman 2001) was used to define a model that classified each pixel to 1 of 12 land cover classes (Figure 3). Random Forests is an ensemble learning algorithm that produces multiple decision trees (50 in this implementation) based on a random subset of the training sample units, and where splits within each decision tree are based on a random subset of the input predictors (Belgiu and Drăgu 2016). When the model is applied to an unclassified pixel, Random Forests will assign the pixel to the land cover class that gets the most votes from all the trees in the ensemble. Random Forests allows for the votes received by each class to be recorded and carried as an additional attribute on the classification output. These votes can be used as analogous to class membership likelihoods, providing enriched information on land cover class uncertainty for use in modeling.

As we used surface reflectance as the source for all our spectral metrics, our land cover classification model, developed using year 2000 data, was considered portable through time (Gómez et al. 2016). Thus for each year in the times series (1984–2012), pixels were labeled with the most voted class (Lawrence et al. 2006; Pal 2005). The result was a preliminary annual land cover classification for each year from 1984 to 2012, according to the 12 classes identified in Figure 3. Of note, to reduce classification confusion, agricultural zones were identified, labeled as herbs, and excluded from further processing and analysis using a mask provided by Agriculture and Agri-Foods Canada (2011 data[1]).

2.5. Time-series post-classification processing

Multi-temporal land cover classification generally results in (i) ecologically unrealistic large levels of year-to-year land cover label change (Abercrombie and Friedl 2016) and in the occurrence of (ii) unlikely land cover transitions (e.g. forested to built-up, and then back to forested) (Clark et al., 2010; Gómez et al. 2016). This implies that further processing in the temporal domain is required to produce coherent multi-temporal land cover layers. To this end, we implemented some specific post-classification steps to stabilize our land cover trajectories and mitigate the potential for unrealistic land cover transitions.

2.5.1. Hidden Markov Model

To distinguish real from spurious land cover changes and produce stable land cover transitions for each pixel through time, we applied a Hidden Markov Model (HMM). HMM is a statistical modeling technique based on state (land cover class, in our case) transition probabilities on a given time-series sequence. An HMM is characterized by 3 probability density functions: the initial state probabilities, the transition probabilities, and the state probabilities. The initial state probabilities density function defines the probabilities that the system is in each state at the initial time. The transition probabilities between states are designed to be dependent on the time interval between the 2 subsequent observations, and are defined by a transition matrix. The state probability density function at each observation time step is based upon the transition probability distribution, which in turn depends on the previous and following states (forward–backward algorithm) (Gader et al. 2001; Lee et al. 2013; Trier and Salberg 2011; Yu 2010).

In each year we defined the initial probabilities for each pixel using the land cover votes generated by the Random Forests model following the approach described in Abercrombie and Friedl (2016). We applied the forward–backward HMM algorithm (Yu and Kobayashi 2006) using transition class probabilities defined based on knowledge of forest vegetation development, as explained below in this section. This resulted in class probabilities

[1] ftp://ftp.agr.gc.ca/pub/outgoing/aesb-eos-gg/CEN_CA_AG_INTRP/AgrMask2011/AgriculturalMask2011_AAFC.gdb.zip

Table 2. Successional land cover transition probability matrix.

		To											
		Water	Snow/Ice	Rock/ Rubble	Exposed/ Barren Land	Bryoids	Herbs	Wetland	Shrubs	Wetland-treed	Coniferous	Broadleaf	Mixedwood
From	Water	0.9	0.025	0.001	0.001	0.001	0.001	0.025	0.001	0.001	0.001	0.001	0.001
	Snow/Ice	0.025	0.9	0.025	0.025	0.001	0.001	0.001	0.001	0.001	0.001	0.001	0.001
	Rock/Rubble	0.001	0.025	0.9	0.001	0.025	0.025	0.001	0.025	0.001	0.001	0.001	0.001
	Exposed /Barren Land	0.001	0.025	0.001	0.9	0.025	0.1	0.001	0.001	0.001	0.001	0.001	0.001
	Bryoids	0.001	0.001	0.001	0.001	0.9	0.001	0.001	0.001	0.001	0.001	0.001	0.001
	Herbs	0.001	0.001	0.001	0.001	0.001	0.9	0.001	0.1	0.001	0.001	0.001	0.001
	Wetland	0.025	0.001	0.001	0.001	0.001	0.001	0.9	0.001	0.1	0.001	0.001	0.001
	Shrubs	0.001	0.001	0.001	0.001	0.001	0.001	0.001	0.9	0.1	0.1	0.1	0.1
	Wetland-treed	0.001	0.001	0.001	0.001	0.001	0.001	0.025	0.001	0.9	0.001	0.001	0.001
	Coniferous	0.001	0.001	0.001	0.001	0.001	0.001	0.001	0.001	0.001	0.9	0.001	0.025
	Broadleaf	0.001	0.001	0.001	0.001	0.001	0.001	0.001	0.001	0.001	0.001	0.9	0.025
	Mixedwood	0.001	0.001	0.001	0.001	0.001	0.001	0.001	0.001	0.001	0.025	0.025	0.9

for each pixel for any given year in the time series. Pixels were then labeled with the most likely land cover class for a particular year. The land cover transition probability matrix defines the probability that a pixel will change between land cover classes from 1 year to another. Our matrix (see below) was defined based on forest succession knowledge, with the premise that stand-replacing changes (i.e., fire and harvesting) reset and reinitiate the successional land cover transitions of forest vegetation development. Thus, stand-replacing disturbances lead to various phases of forest vegetation development following disturbance, including the establishment and regeneration phase, young forest regrowth phase, mature and transition phase, and old-growth phase (Bartels et al. 2016; Oliver 1981). The transition probability matrix is presented in Table 2 and scores the land cover transition probabilities as likely (0.90), probable (0.10), possible (0.025), or not likely (0.001); see Gómez et al. (2016) for information regarding transition probabilities. We defined stable cases where the land cover stays unchanging from year to year as the most likely situations (Pouliot et al. 2014). "Probable" transitions comprise forest vegetation development successions. "Possible" transitions are those land cover changes that are less frequent in the frame of a vegetation successional environment, but can still happen. "Not likely" transitions are defined for unexpected land cover conversions (Gómez et al. 2016). Forest changes informed land cover transitions. Thus, we considered the stand-replacing changes (i.e., fire, harvesting) determined by C2C forest change attribution product (Hermosilla et al. 2016) as *hard lines* in the transition probabilities. This implied that the temporal dependency between land covers defined by the successional transition probabilities was broken in the years before and after a change event. In practice, this worked as a piecewise application of the HMM, where the land cover transition probability matrix was independently applied to the temporal segment defined by the stand replacing changes.

2.5.2. Logical land cover transition rules

In this step, we focused only on the unlikely land cover transitions. Although theoretically a wide variety of land cover transitions may be possible, there are natural and logical limitations that may be used to improve the accuracy of the land cover classification process (Liu and Zhou 2004). In this sense, unlikely land cover transitions were constrained by exploiting the temporal consistency of pixels in the same location through time (Pakzad 2002; Radke et al. 2005). Land cover transition rules based on prior knowledge can be defined to restrict unlikely land cover transitions (e.g. Bater and Coops 2011; Clark et al. 2010; Liu and Cai 2012). We defined transition rules to prevent the presence of water after fire wildfire events, snow/ice after harvesting events, and rock/rubble after both wildfire and harvest.

2.6. Land cover validation

Following the sampling methodology identified in Wulder et al. (2007) we implemented a stratified random sampling approach to select validation points from high spatial resolution imagery. A common challenge of time series land cover information is validation (Gómez et al. 2016). Based on our use surface reflectance, and the concomitant portability of our land cover model, we chose to validate a single annual land cover map as per Franklin et al. (2015). The year 2005 was selected for validation as it was the year with the greatest number of high spatial resolution satellite images (QuickBird) available in Google Earth™, which was the primary reference data source for validation. For the response design, each land cover class was considered as a stratum, and sample units were randomly selected from each stratum. An overall sample size of 1,200 was selected using Equation 1 (Cochran 1977).

$$n = \left[\left(\frac{z}{m}\right)^2\right] \times p \times (1-p) \quad (1)$$

Table 3. Validation sample allocation.

Stratum (Class)	Area (ha)	% of total area	Number of sample units	Sample covered area (ha)	% of total sample units
Water	67,882,738	10.5	113	10.2	9.4
Snow/ice	7,117,227	1.1	57	5.1	4.8
Rock/rubble	5,402,063	0.8	55	5.0	4.6
Exposed/barren land	29,265,355	4.5	77	6.9	6.4
Bryoids	26,738,981	4.1	75	6.8	6.3
Shrubs	79,275,896	12.3	123	11.1	10.3
Wetland	68,361,181	10.6	113	10.2	9.4
Wetland treed	51,173,510	7.9	97	8.7	8.1
Herbs	39,370,513	6.1	86	7.7	7.2
Coniferous	183,706,722	28.4	220	19.8	18.4
Broadleaf	29,055,368	4.5	77	6.9	6.4
Mixedwood	59,461,401	9.2	105	9.5	8.8

where n is the total sample size, z is the percentile of the standard normal (1.96 for 95% confidence interval), m is the margin of error (0.02), and p is the assumed population proportion (0.85).

As per Czaplewski and Patterson (2003), we allocated half of the sample units proportional to the area of each land cover stratum in 2005, and allocated the remaining half to improve estimates for rare classes using Equation 2.

$$n_i = \left[p_i \times \left(\frac{n}{2}\right) + \left(\frac{1}{k}\right) \times \left(\frac{n}{2}\right) \right] \qquad (2)$$

where n_i is the sample size allocated to stratum i, p_i is the proportion of the total area mapped as i, n is the total sample size, and k is the number of land cover classes (12). The final sample allocation is presented in Table 3. To address concerns of spatial autocorrelation, we checked the minimum distances between sample units to ensure each sample was ≥500 m from the nearest sample unit. No sample units were found to violate this assumption, so no remedial action was required.

For the evaluation protocol, a spatial support region approximately equivalent to a 30-m pixel was used for interpretation and was defined by buffering each sample point by 17 m. Each sample was manually interpreted from the high spatial resolution imagery by the same interpreter, who was trained to visually recognize the land cover types using a reference interpretation key as a guide. The interpreter was instructed to identify the most likely class, with an option to also specify a second choice if there were clearly 2 dominant lands covers found within the spatial support region and/or if the sample fell within a transition zone between land cover classes. The use of second choice accommodates both thematic ambiguity and spatial accuracy (Stehman and Czaplewski 2003). Agreement was defined if the predicted class for 2005 matched either the interpreter's primary or secondary land cover class. The results of the accuracy assessment were then summarized in a confusion matrix based on estimated class area proportions, from which overall accuracy, and user's and producer's accuracies for each class were computed as well as 95% confidence intervals (Olofsson et al. 2014).

2.7. Assessing the impact of post-classification processing

We assessed the effect of HMM by mapping and reporting on the number of per-pixel land cover transition predictions resulting from the preliminary annual land cover classification, and following the post-classification process. To provide additional insight on the classifications generated, we tested the attribution confidence of the pixels whose class was modified by the HMM and compared them to the pixels where the class was not modified. We used the distance to second voted class by the Random Forests classifier as indicator of attribution confidence (Mitchell et al. 2008). This confidence indicator is computed using Equation 3:

$$C = 1 - \frac{v_2}{v_1} \qquad (3)$$

where v_1 is the proportion of votes of the assigned class and v_2 is the proportion of votes of the second most voted class. The values of C range between 0 (low confidence attributions) and 1 (high confidence attributions).

3. Results

3.1. Impacts of post-classification processing

The per-pixel distribution of land cover transitions resulting from the initial, annual, land cover classifications is shown in Figure 4a (recalling that agricultural areas have been masked). The map shows a large number of transitions across the boreal forest, in contrast with mountainous areas on the west coast and eastern Quebec. As a result of the HMM post-classification process (Figure 4b), the number of land cover transitions is notably reduced across Canada, with the pixels that persist with greater numbers of transitions distinguishable at this scale located in the areas more prone to wildfires. We also produced cumulative histograms comparing the

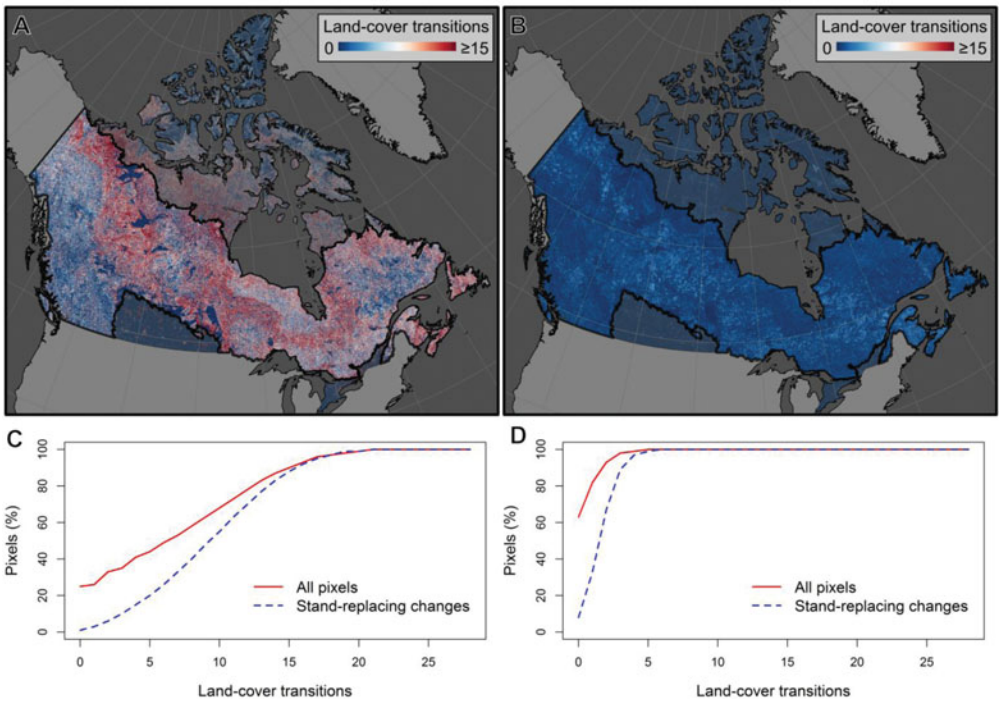

Figure 4. Number of land cover transitions before (a) and after (b) time series post-processing; and cumulative histograms of the number of land cover transitions for all pixels and pixels with stand-replacing changes (fire and harvesting detected with the C2C approach, (Hermosilla et al. 2016)) before (c) and after (d) time series post-processing.

frequency of land cover transitions for all pixels and for those pixels with stand-replacing changes before (Figure 4c) and after the post-processing (Figure 4d).

The initial annual land cover classification resulted in a majority of pixels frequently changing their land cover class across the analyzed period, with an average of 7.1 transitions ($\sigma = 6$) per pixel. 44% of the pixels accounted for ≤5 transitions and 25% presented no land cover changes. The use of HMM in the post-classification processing resulted in 0.6 transitions ($\sigma = 1$) on average per pixel. 63% of the pixels presented no land cover changes, and only 0.04% of the total population exhibited more than 5 transitions. Pixels undergoing stand-replacing changes along the analyzed period (8.8% of the total) had on average 9.8 ($\sigma = 4.7$) initial land cover transitions, which resulted in 2.1 ($\sigma = 1.2$) transitions following the application of HMM. Figure 5 compares the attribution confidence distribution of pixels which class was modified and not modified by the HMM process. Pixels where the land cover class was not modified were attributed with higher confidence (median = 0.80) than those pixels modified by the post-processing (median = 0.36), and only 5.9% of the modified pixels presented confidence attributions >0.80.

3.2. Land cover validation results

The annual land cover output for 2005 was evaluated using independent reference data. The resulting confusion matrix for the preliminary land cover classification considering all 12 classes is shown in Table 4, and the assessment of the HMM post-processed classification is shown in Table 5. The results indicated that the application of the HMM improved the classification by increasing the overall accuracy from 64.7% (95% confidence interval ± 2.7%) in the preliminary classification to 70.3% (± 2.5%) in the post-processed land cover product. This overall accuracy value is partially boosted by the higher accuracies of spectrally distinct classes, such as snow and

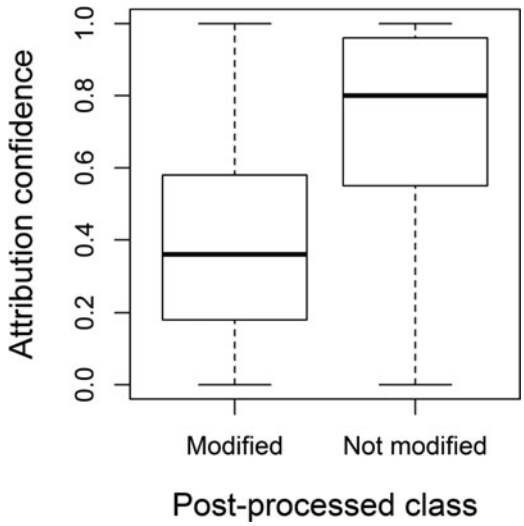

Figure 5. Box-and-whisker plots showing median, interquartile range, and extreme values of the attribution confidence of pixels where the land-cover class has been modified or not by the post-processing process.

Table 4. Confusion matrix of preliminary land cover classification for 2005 populated by estimated proportions of area, with 95% confidence intervals.

	Reference													
	Water	Snow/Ice	Rock/ Rubble	Exposed/ Barren Land	Bryoids	Herbs	Wetland	Shrubs	Wetland -treed	Coniferous	Broadleaf	Mixedwood	Total	User's accuracy (%)
Water	0.0923	0	0.0007	0	0.0007	0.0007	0.0007	0	0.0014	0.0028	0.0007	0	0.10	92 ± 4
Snow/Ice	0	0.007	0.0012	0	0.0005	0.0005	0.0002	0.0002	0	0.0002	0	0.0002	0.01	70 ± 12
Rock/Rubble	0	0	0.0082	0	0.0006	0.0002	0.0004	0.0004	0	0	0.0002	0	0.01	82 ± 11
Exposed/Barren Land	0.0016	0.0005	0.0121	0.0174	0.0063	0.0032	0.0011	0.0037	0.0011	0.0021	0	0.0011	0.05	35 ± 10
Bryoids	0	0	0.0005	0.0014	0.0098	0.0019	0.0158	0.0042	0.0033	0.0019	0.0005	0.0009	0.04	24 ± 9
Herbs	0	0	0.0006	0.0013	0.0013	0.0417	0.0019	0.0082	0	0.0013	0.0025	0.0013	0.06	69 ± 9
Wetland	0.0009	0	0.0009	0.0009	0.0034	0.0017	0.0627	0.0069	0.0155	0.0129	0	0.0043	0.11	57 ± 9
Shrubs	0.0019	0	0.0009	0.0028	0.0074	0.0056	0.0074	0.0642	0.0047	0.0093	0.0084	0.0074	0.12	53 ± 9
Wetland treed	0.002	0	0	0	0.0007	0	0.0079	0.0079	0.042	0.0111	0.0026	0.0059	0.08	52 ± 9
Coniferous	0.0033	0	0	0.0033	0	0	0.0066	0.0116	0.0149	0.2088	0.0116	0.0199	0.28	75 ± 7
Broadleaf	0.0006	0	0	0	0	0.0006	0.0006	0.0041	0.0012	0.0029	0.022	0.0081	0.04	55 ± 12
Mixedwood	0.0009	0	0	0	0	0.0017	0.0026	0.0034	0.0017	0.0094	0.006	0.0643	0.09	71 ± 9
Total	0.10	0.01	0.03	0.03	0.03	0.06	0.11	0.11	0.09	0.26	0.05	0.11		
Producer's accuracy (%)	89 ± 5	93 ± 8	33 ± 11	64 ± 14	32 ± 12	72 ± 9	58 ± 8	56 ± 8	49 ± 9	79 ± 6	40 ± 11	57 ± 9		
Overall accuracy	**64.7% ± 2.7%**													

Table 5. Confusion matrix of post-processed land cover classification (post-Hidden Markov Models) for 2005 populated by estimated proportions of area, with 95% confidence intervals.

	Reference													
	Water	Snow/ Ice	Rock/ Rubble	Exposed/ Barren Land	Bryoids	Herbs	Wetland	Shrubs	Wetland -treed	Coniferous	Broadleaf	Mixedwood	Total	User's accuracy (%)
Water	0.0935	0	0.0014	0	0.0007	0.0007	0	0	0	0.0029	0.0007	0	0.10	94 ± 4
Snow/Ice	0	0.0062	0.0018	0	0.0005	0.0008	0.0002	0.0005	0	0	0	0.0002	0.01	62 ± 12
Rock/Rubble	0	0	0.0087	0	0	0.0002	0.0002	0.0004	0	0.0004	0	0	0.01	87 ± 10
Exposed/Barren Land	0.0022	0.0011	0.0089	0.0183	0.0083	0.0033	0.0017	0.0033	0.0006	0.0011	0	0.0011	0.05	37 ± 10
Bryoids	0	0	0.0005	0.0025	0.011	0.0015	0.017	0.002	0.003	0.0015	0.0005	0.0005	0.04	28 ± 10
Herbs	0	0	0	0.0013	0.0013	0.0458	0.0007	0.0061	0	0.0013	0.002	0.0013	0.06	76 ± 9
Wetland	0.0016	0	0.0008	0	0.004	0.0016	0.0701	0.004	0.0143	0.0112	0	0.0024	0.11	64 ± 8
Shrubs	0.0017	0	0	0.0025	0.0076	0.0025	0.0068	0.071	0.0051	0.0144	0.0034	0.0051	0.12	59 ± 8
Wetland treed	0.0007	0	0	0	0	0	0.005	0.0065	0.0461	0.0151	0.0022	0.0043	0.08	58 ± 9
Coniferous	0.0063	0	0	0.0021	0	0	0.0042	0.0063	0.0084	0.234	0.0084	0.0104	0.28	84 ± 6
Broadleaf	0	0	0	0	0	0.001	0.0005	0.0047	0.0021	0.0021	0.026	0.0036	0.04	65 ± 11
Mixedwood	0.0013	0	0	0	0	0.0013	0.0027	0.0027	0.0013	0.0113	0.0047	0.0647	0.09	72 ± 8
Total	0.11	0.01	0.02	0.03	0.03	0.06	0.11	0.11	0.08	0.3	0.05	0.09		
Producer's accuracy (%)	87 ± 6	85 ± 11	39 ± 11	68 ± 14	33 ± 12	78 ± 9	64 ± 8	66 ± 8	57 ± 10	79 ± 6	54 ± 12	69 ± 8		
Overall accuracy	**70.3% ± 2.5%**													

water. On the other hand, classes with spectral overlap resulted in the lowest (bryoids) and more unbalanced (rock/rubble, exposed/barren land) user's and producer's accuracies. Within the treed classes, the wetland-treed class had the smallest user's and producer's accuracies, while the coniferous class had the largest values. Using the HMM post-processing, overall accuracy at the most generalized level of the land cover classification hierarchy (Figure 3; land-base level: vegetated vs. non-vegetated) was 94.8% (± 1.2%). At the subsequent land-cover level (Figure 3; non-vegetated, vegetated non-treed, vegetated treed), the overall accuracy was 82.5% (± 2.1%).

3.3. Annual land cover maps

We produced Canada-wide annual land cover thematic maps for 1984–2012 following the change-informed time-series land cover classification framework introduced here. The land cover classification map for 2005 is shown in Figure 6 as an example. To produce these time-consistent land cover products, we used the votes of the Random Forests model as class likelihood in the Hidden Markov Model. The class likelihoods in 2005 for the 12 land covers considered are shown in Figure 7. Mapping these likelihoods can offer further insights and enrich the classifications results.

3.4. Characterization of Canada forested-ecosystem's land cover dynamics from 1984–2012

From the annual land cover maps, we summarized the land cover distribution and dynamics information for Canada forested-ecosystem's (comprising 649,981,522 ha, as reported by White et al. 2017) between 1984 and 2012 (Table 6 and Figure 8). On average, coniferous is the most common land cover (29.2%), followed by shrub (11.7%), wetland (10.8%), and water bodies (10.5%). Rock/rubble (0.9%) and snow/ice are markedly less frequent land cover categories. Coefficient of variation values were under 0.1 for every land cover type, with broadleaf (0.09) and bryoids (0.08) as the most variable classes, and water (0.001) as the most stable land cover. Figure 8a shows the land cover distribution annually in the forested ecosystems.

Table 6. Summary of relative distribution of land cover per class in the forested ecozones of Canada for 1984–2012.

Class	Minimum (%)	Maximum (%)	Mean (%)	St. deviation (%)	Coefficient of Variation (%)
Water	10.50	10.58	10.54	0.02	0.001
Snow/Ice	1.11	1.32	1.18	0.05	0.04
Rock/Rubble	0.81	1.00	0.87	0.05	0.06
Exposed/Barren	4.35	5.31	4.69	0.25	0.05
Bryoids	4.18	5.21	4.53	0.38	0.08
Herb	5.83	7.02	6.21	0.29	0.05
Wetland	10.10	11.81	10.81	0.46	0.04
Shrub	10.79	12.80	11.67	0.71	0.06
Wetland-Treed	6.80	8.93	7.69	0.48	0.06
Coniferous	28.38	30.52	29.16	0.72	0.02
Broadleaf	3.67	4.78	4.16	0.38	0.09
Mixedwood	7.65	9.28	8.48	0.57	0.07

Land cover dynamics before and after the stand-replacing change events caused by harvesting and fire are shown in Figure 8b and Figure 8c, respectively. These figures uniquely represent the area affected by harvesting, which represented 16,856,857 ha or 2.59% of Canada's forested ecozones, and wildfires, which represented 40,627,872 ha or 6.25% of Canada's forested ecozones, as reported by White et al. (2017). Note that the sample population across the analyzed period is variable, with a greater number of pixels with a shorter time since disturbance and a lesser number of pixels with longer periods of time since disturbance. The sample population is indicated by the respective histograms representing the percentage of pixels used to generate the land cover distribution at each time step. This distribution produces more unstable trends at the beginning and end of the analyzed period (i.e., in the tails of the distribution). Thus, results produced with lower pixel populations are noted and consequently more cautiously interpreted.

The pre-harvesting scenario (Figure 8b) is clearly dominated by treed classes (i.e., wetland-treed, coniferous, broadleaf, and mixedwood) and coniferous is markedly the most common class (60%). Harvest activities result in a mosaic of land cover types post-disturbance, principally composed of exposed/barren land, herbs and shrubs, immediately following the change event. As the time since disturbance increases, the presence of these land cover classes is gradually reduced and replaced by treed classes. Thus, right after the disturbance treed land cover classes account for 6% of pixels, while >20 years after disturbance on average, treed classes account for 78% of pixels. Harvesting entails a change on the tree species distribution in comparison with this early pre-disturbance scenario, with increased presence of mixedwood and broadleaf classes in the years following the harvest event. An example of the land cover dynamics following harvesting events is displayed in Figure 9a.

Before wildfire events (Figure 8c), treed classes account for 71% of disturbed pixels. Coniferous is the most frequent land cover class (57%), and wetlands (15%) and shrubs (6%) are the most frequent non-treed classes affected by fires. Fires result in a major removal of vegetation. Immediately after wildfire events, the majority of pixels belong to exposed/barren land (58%) and

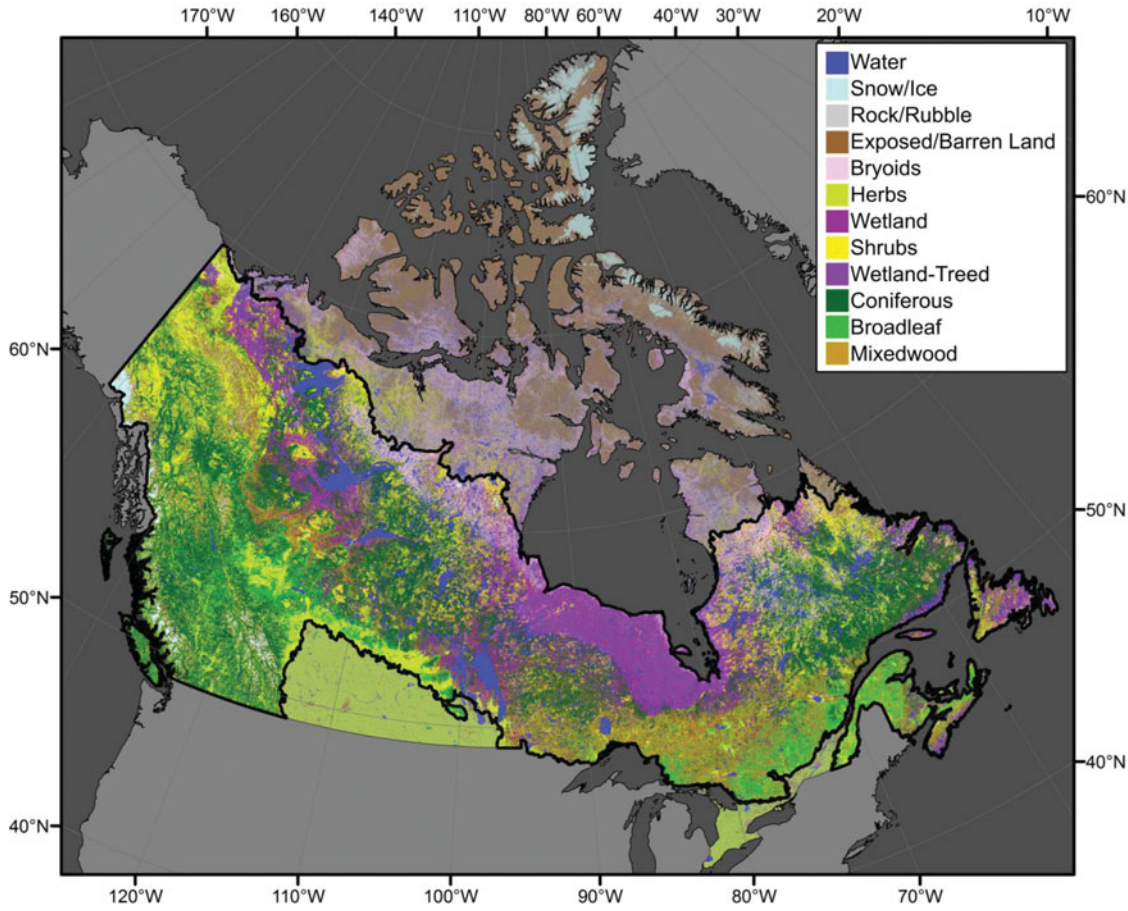

Figure 6. Resulting land cover classification map of Canada for the year 2005.

shrub (23%) classes. In the years following the disturbance event, the presence of treed-class pixels gradually increases, at a considerably lower rate than after harvesting events. Thus, 1 year after the fire, treed classes account for 7% of the pixels, while 20 years after a wildfire, treed classes account for 36% of pixels. These results echo the differences in post-disturbance recovery trends reported for harvest and wildfire by White et al. (2017). Figure 9b shows an example of land cover succession after a wildfire event.

4. Discussion

In this research, we presented the Virtual Land Cover Engine—a spatially extensive, temporally dense, and flexible framework for the mapping of land cover. The VLCE framework combines a time series of image classifications and disturbance information, with knowledge of ecological succession to produce temporally consistent maps of land cover from time series of Landsat surface-reflectance image composites. A key aim of the VLCE framework is to be flexible to differing data inputs, with map quality assessed using a robust sampling design and independent validation data. We demonstrated this methodological framework by producing annual 30-m Canada-wide land cover maps from 1984 to 2012, and describe the land cover dynamics in the forested ecosystems of Canada, with special focus on land cover following wildfire and harvest events.

4.1. Nature of data inputs and outputs: Flexibility of the VLCE framework

The land cover classification framework herein presented is transferable to other regions or ecosystems, adaptable to suitable training datasets, and flexible in the definition of land cover categories for a range of user needs and focus domains. This suite of VLCE framework traits is aimed to offer flexibility in map production and to accommodate a diversity of user-focused features of land cover map development and application as outlined by Comber et al. (2005). We applied this framework to Canada's forested ecosystems as proof-of-concept. While the Landsat archive over Canada is plentiful both over space and time (White and Wulder 2014), the number of available observations in some cases is more limited in other regions and nations globally (Wulder et al. 2016).

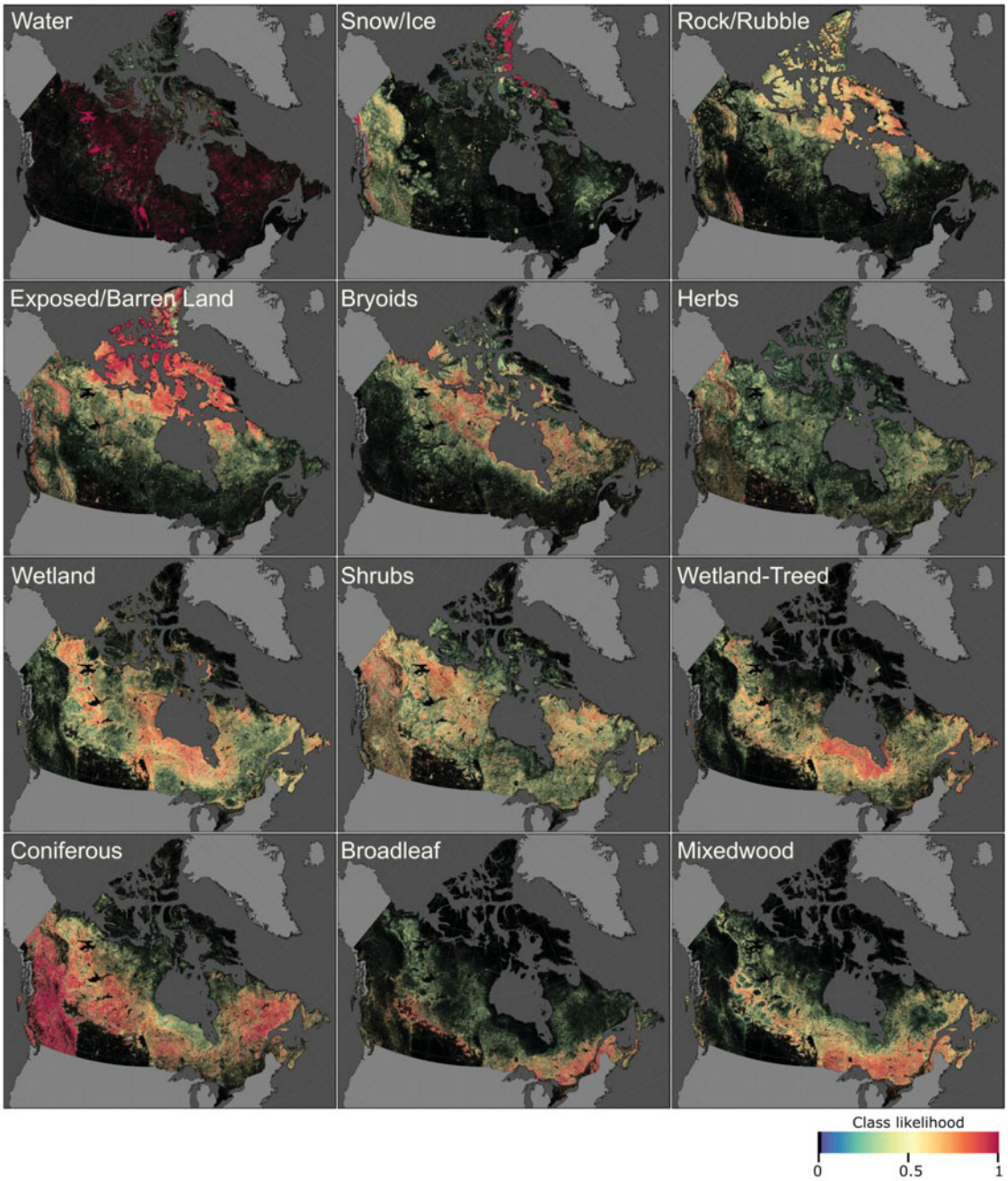

Figure 7. Land cover classification likelihoods obtained from the Random Forests votes for the year 2005.

Since access to suitable training observations for large and remote areas that are comparable through time is challenging, there are an increasing number of studies that derive training data from pre-existing land cover products (Inglada et al. 2017; Wessels et al. 2016; Zhang and Roy 2017; Zhu et al. 2016). In this research, we used a land cover product representing c. 2000 conditions (Wulder et al. 2008). An existing land cover classification may not be optimal training data, since its inherent error can be propagated to the resulting land cover products. However, pre-existing land cover maps do provide for a large number of training sample units across a broad range of spectral conditions, and allow for an improved representation of sample units across the feature space, both factors that are important for classifiers such as Random Forests (Belgiu and Drăgu 2016). Recently, Pelletier et al. (2017) reported that Random Forests classifier is not negatively impacted by low levels of random noise in training data (up to 30%, in some configurations); importantly, they also stress the impact that noisy training data can have on out-of-bag (OOB) error assessments. These findings further support the importance of independent validation data and assessment procedures and to not rely on OOB assessments to relate map quality.

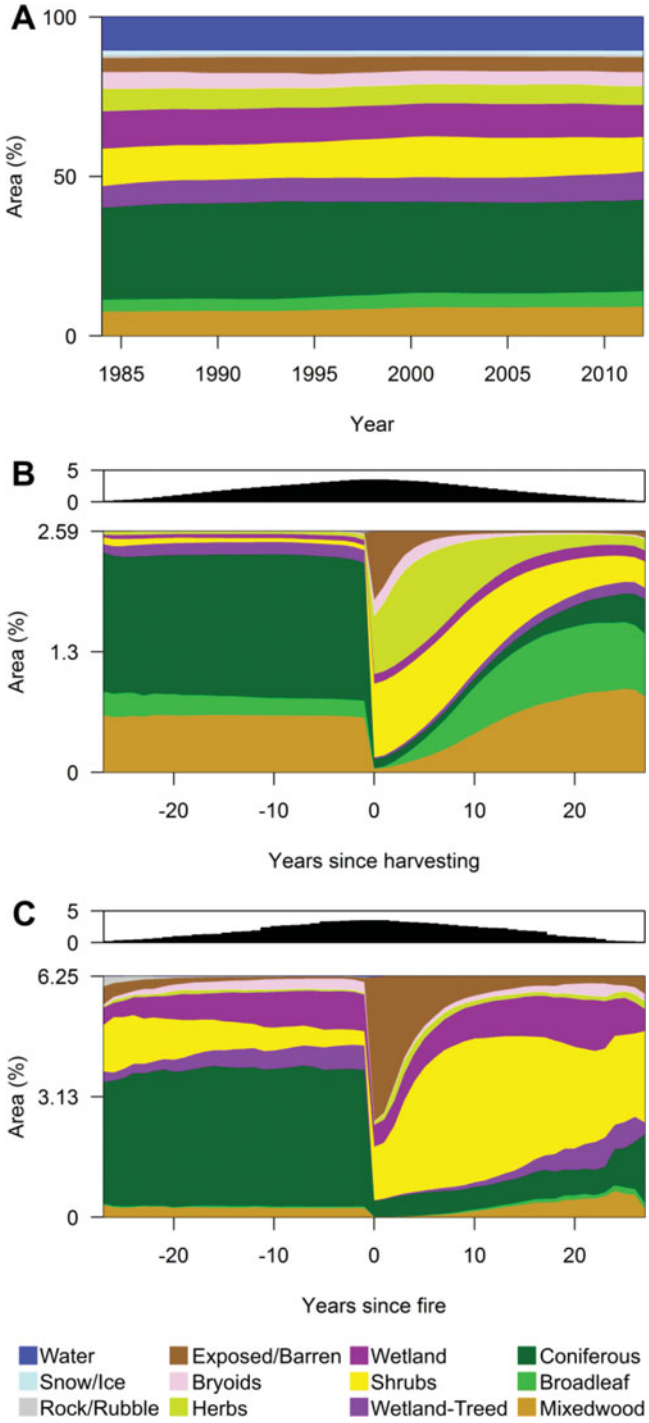

Figure 8. Land cover distribution in (a) Canada's forested ecosystems from 1984 to 2012, and before and after (b) harvesting and (c) wildfire change events detected with the C2C approach (Hermosilla et al. 2016) over all Canada. Histograms show the sample population (i.e., percentage of pixels) through time.

As a component of the VLCE framework, class membership likelihood maps are generated (Figure 7). These class membership likelihoods served to inform post-classification procedures (see below) and also provide a unique source of independent mapping information. The spatial trends present in class membership likelihoods have a spatial cohesion to the mapped features. Conceptually, these class likelihoods are similar to the "distance to second cluster" metric put forward by Mitchell et al. (2008).

It is worthwhile to note that many applications require relatively generalized land cover masks to enable modeling or stratification layers to constrain analyses or for reporting activities (White et al. 2014). In the case of the mapping outcomes related here, we report accuracies for relaying higher-order summaries of the land cover classification system used, for example treed versus non-treed (82.5%) and vegetated versus non-vegetated (94.8%). As noted by others, accuracies for land cover products typically increase with increasing levels of generalization (Remmel et al. 2005). These more generalized land cover outputs provide additional information products of use for a variety of applications.

4.2. Post-classification processing

The use of the annual gap-free, seamless, Landsat surface reflectance composites produced following the C2C protocol (Hermosilla et al. 2016) promotes the spatial continuity of the land cover product generated with the VLCE framework. Prior to the opening of the USGS Landsat archive in 2008, land cover products often required the use of images from different seasons or multiple years in order to realize the required spatial coverage for a single-year land cover map, and despite these efforts, often included areas with persistent data gaps (Vogelmann et al. 2001; Wulder et al. 2008). The VLCE framework enables the simultaneous generation of a series of annual land cover maps, thereby ensuring temporal consistency both in land cover transitions and technical specifications (e.g., spatial resolution, land cover classes). Land cover products intended to update earlier versions of remote-sensing land cover maps were generally designed to take advantage of methodological and technological advances, while at the same time maintaining reasonable compatibility with the initial version (EEA 2002; Homer et al. 2004). During those updating processes, change detection methods were generally used to bound the potential areas to be relabeled, limiting the spatial extent of the new classifications (Xian et al. 2009).

In the VLCE, forest change data is used in combination with known ecological succession processes to inform the land cover transition process. This improves the temporal consistency of the annual land cover products, and prevents ecologically unrealistically high levels of year-to-year land cover change that can often result with post-classification comparison (see Fuller et al. 2003). In the VLCE framework, we used HMM, which rely on spectral evidence of land cover types provided by initial

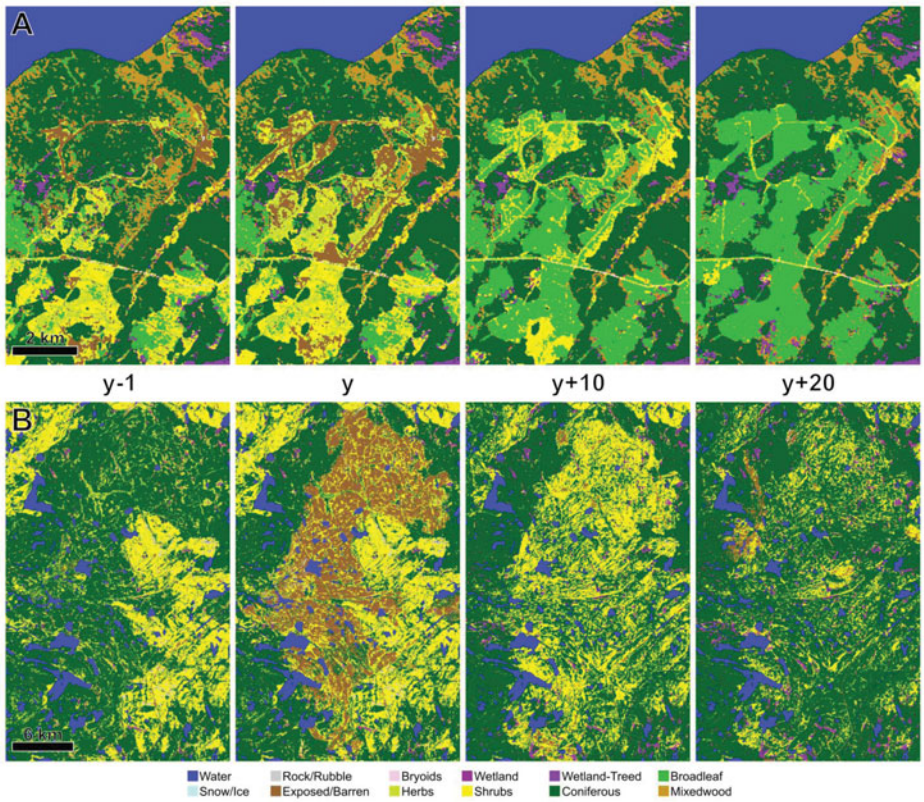

Figure 9. Examples of land cover sequence before and after (a) harvesting and (b) fire change events; y represents the year of change.

probabilities of a Random Forests model, to define land cover changes (Abercrombie and Friedl 2016). HMM primarily focus on pixels with low confidence and modify the attributed land cover class (Figure 5), resulting in a reduction in the number of spurious land cover transitions. As a result, HMM precludes the need to specify elaborate rules governing all possible class transitions. We therefore restricted our use of transition rules to avoid very unlikely land cover transitions resulting from known spectral confusion, such as burned areas misclassified as water (Frolking et al. 2009).

4.3. *Land cover dynamics over Canada's forested ecosystems*

Overall, the land cover distribution in Canada's forest ecosystems remains largely stable through time (Figure 8a), and the distribution of land cover categories exhibits limited variability at this scale (Table 6). Post-disturbance trends in successional development are evident. Our land cover cube demonstrates how stand-replacing disturbances alter the relative proportions of forest type composition with regards to the pre-change scenario. Thus, while coniferous forest is the most frequently harvested land cover class in Canada (Figure 8b), broadleaf and mixedwood types can be more prevalent post-harvest. While some harvested areas are replanted with coniferous species in the years immediately following harvesting; other areas are left to regenerate naturally and the dominance of coniferous species might be delayed, followed instead by the transition from initial herb and/or shrub vegetation, to deciduous, and then gradually to coniferous (Oliver 1981). Moreover, harvesting activities can leave a significant amount of residual forest on site, including advanced regeneration (tree seedlings and saplings) and also mature seed trees (Jarron et al. 2017; Seedre et al. 2014). Similarly, after wildfires there is an increasing relative dominance of mixedwood forest and– to a lesser extent– broadleaf, compared with the pre-fire distribution (Figure 8c). Traditionally post-fire dynamics are summarized as gradual transition of broadleaf species by mixedwood, and then coniferous stands (Bergeron and Harvey 1997). Nevertheless, this idealized transition varies depending on both the nature of the disturbance, and the composition of the disturbed forest stand and its surroundings (e.g., soil moisture, climate) (Bergeron et al. 2014; Johnstone et al. 2010). With under 10% of Canada's forested ecosystems subject to stand replacing disturbance, via harvest or fire, during the near 3-decade analysis period, natural ecosystem processes are dominant over the majority of the ~ 650 million ha region of analysis. These natural ecosystem processes can include stable non-vegetated features (e.g., water, rock/rubble), stable vegetated features (e.g., climax shrubs, bryoids),

through to the successional processes active over treed lands (e.g., maturing forest). The land cover present early in the time series are the product of previous disturbances and ongoing successional processes. Figure 8b and Figure 8c illustrate the nature of successional development over time that can be expected for each disturbance type. Plus, the pre-disturbance conditions relate the nature of the land cover present, ongoing successional insights, and the developments from disturbances occurring before the dates captured in this study. The harvesting of mature forests and the return to forest land cover categories on productive sites is well related in Figure 8b. The more categorically broad impacts present related to wildfire are evident in Figure 8c, with the land cover transitions present beginning to resemble the pre-disturbance land cover conditions over time.

4.4. Time-series land cover insights and considerations

We presented a framework to produce an annual land cover classifications for a near 3-decade period. The integrity of the land cover maps over time is achieved by considering the annual land cover as temporal steps in a data cube. Each individual element (year) of the cube independently has the utility and functionality of a traditional single-year land cover map. The disturbance-informed nature and the ecological-succession processes based on annual membership likelihood values inform the land cover transition process. Changes in land cover over time are present through both change detection procedures (largely focused on depletions) and successional development over time. Our results illustrate that when used with the HMM, the annual likelihood values serve to improve both map accuracy and the temporal consistency of land cover products. In addition, annual likelihood values provide spatially explicit information useful for refined mapping of individual classes, offering further local information for specific classes and as understood over sub-regions of interest, with unique and enhanced modeling opportunities possible beyond purely categorical classification outcomes (Khatami et al. 2017).

Approaches that integrate temporal information in the land cover classification process have been demonstrated as superior to single-date methods (Gómez et al. 2016). In the framework presented herein, the temporal domain is incorporated by integrating forest disturbance information and ecological succession knowledge plus the HMM over preliminary land cover classification results produced with Random Forests. Other strategies to integrate the temporal domain of annual time series may involve analyzing the spectral values of pixels through time to inform land cover change transitions during the attribution process or in a post-classification step (Franklin et al. 2015). This implies partitioning those temporal trajectories into linear segments (as per Kennedy et al. 2010) which are individually described via spectro-temporal metrics describing the duration (i.e., long term, short term) and the magnitude (i.e., subtle, abrupt; Hermosilla et al. 2015a) for characterizing vegetation stability, change, and recovery (Gómez et al. 2016).

The VLCE framework was tested over Canada's forested ecosystems, where an annual frequency is an appropriate analysis period for capture of the dominant disturbance processes. Further, the annual frequency aids in image compositing through enabling an acquisition window large enough for the necessary data yield without introducing phenological artifacts (White et al. 2014). Also noted in White et al. (2014) is that different information needs or ecosystems (and disturbance or management processes present) may require different image processing and analysis strategies. For instance, regions subject to agricultural activities could benefit from finer analysis frequencies (i.e., seasonal, monthly) and the development of agricultural specific land cover transition probabilities.

The analysis span considered (1984–2012) limits the depiction of post-disturbance vegetation development to initial stages of post-disturbance regrowth, with a maximum period of 28 years. Note that collection of 30 m Landsat measures commenced in 1982 with Landsat-4 MSS, although coverage was initially sparse (Wulder et al. 2015). With the launch of Landsat-5 TM in 1984, the era with increasingly broad global coverage of 30-m Landsat begins. Based upon spatial and temporal image coverage for Canada (White and Wulder 2014), national wall-to-wall analysis based upon calibrated surface-reflectance Landsat-5 TM and -7 ETM+ data is possible from 1984 onwards. Now designated as operational programs, Landsat-8 OLI and Sentinel-2 are expanding the observation period up to the present day (Hermosilla et al. 2017; Roy et al. 2014; Wulder et al. 2015). Retrospectively, there is also potential to integrate Landsat MSS data (Braaten et al. 2015) to characterize conditions prior to 1984. Incorporation of Landsat MSS data would serve to extend the length of time-series land cover information products back to 1972, providing a longer baseline for understanding forest dynamics, including disturbance regimes and subsequent forest recovery. From a land cover perspective, the differing spectral content and coarser spatial resolution of the MSS can be expected to reduce the effectiveness of spectral classifiers and capacity for detecting change. Landsat MSS data combined with the 30-m era imagery, and image processing and

backcasting may be used to inform on broad scale change and aid in generation of land cover (Gómez et al. 2016).

5. Conclusions

There is an increasing need for automated methods that exploit the open access to Landsat time-series data to meet the broad demand for land cover products. Mapping and quantifying land cover changes is critical for ecosystem monitoring. Disturbance informed annual land cover maps provide valuable information on land cover dynamics at a spatial and temporal resolution suitable to monitor both natural and anthropogenic changes in forested and other ecosystems. Thematic annual land cover products provide a practical implementation for science-based support of a wide range of objectives, such as systematic monitoring and subsequent reporting on historic land cover patterns that are otherwise difficult to obtain from non-harmonized products. Having an approach that is flexible to data inputs and that can be implemented utilizing high-performance computing allows for exploiting a range of purpose collected or pre-existing training data sources. The annual national land cover data cube produced with the Virtual Land Cover Engine framework presented herein constitutes valuable information for enhancing Canada's National Forest Inventory and Carbon Accounting programs as well as supporting sustainable forest management activities. Through the VLCE framework, we presented a methodology to produce annual land cover maps informed by disturbance events, controlled for logical transitions, and that queries year-on-year class membership likelihoods via a Hidden Markov Model to reduce the presence of superfluous land cover class transitions. The disturbance-informed annual land cover classification framework presented is flexible to differing calibration data inputs (and related legends) to meet disparate mapping objectives and the interests of different user communities.

The proposed methodology was applied over Canada-wide annual gap-free surface reflectance composites, and forest change and change type attribution layers produced with the Composite-2-Change (C2C) approach. Land cover changes and class transitions resulting from disturbance events are identified as key attributes for carbon modeling (White et al. 2014). The use of annual time-consistent land cover products can contribute to avoid simplistic "from–to" land cover changes by providing a comprehensive land cover evolution of a pixel through time. The resulting 30-m annual land cover cube provides detailed information on the land cover dynamics and forest development following disturbance events to support science-based policies and forest inventory activities, as well as the enrichment of carbon accounting and forest management programs.

Acknowledgments

This research was enabled in part by support provided by WestGrid (www.westgrid.ca) and Compute Canada (www.computecanada.ca). Special thanks to S. Parker Abercrombie (Jet Propulsion Laboratory, NASA) for kindly sharing his HMM code (cited below). We appreciate the time, effort, and insight offered by the journal editors and reviewers.

Funding

This research was undertaken as part of the "National Terrestrial Ecosystem Monitoring System (NTEMS): Timely and detailed national cross-sector monitoring for Canada" project jointly funded by the Canadian Space Agency (CSA), Government Related Initiatives Program (GRIP), and the Canadian Forest Service (CFS) of Natural Resources Canada. Support was also provided by a Natural Sciences and Engineering Research Council of Canada (NSERC) grant to Nicholas Coops.

ORCID

Txomin Hermosilla http://orcid.org/0000-0002-5445-0360
Michael A. Wulder http://orcid.org/0000-0002-6942-1896
Joanne C. White http://orcid.org/0000-0003-4674-0373
Nicholas C. Coops http://orcid.org/0000-0002-0151-9037

References

Abercrombie, S. P., and Friedl, M. A. 2016. *Improving the Consistency of Multitemporal Land Cover Maps Using a Hidden Markov Model*, Vol. 54(No. 2): pp. 703–713

Azzari, G., and Lobell, D. B. 2017. "Landsat-based classification in the cloud: An opportunity for a paradigm shift in land cover monitoring." *Remote Sensing of Environment*, Vol. 202: pp. 64–74. doi:10.1016/j.rse.2017.05.025.

Bartels, S. F., Chen, H. Y. H., Wulder, M. A., and White, J. C. 2016. "Trends in post-disturbance recovery rates of Canada's forests following wildfire and harvest." *Forest Ecology and Management*, Vol. 361: pp. 194–207. doi:10.1016/j.foreco.2015.11.015.

Bater, C. W., and Coops, N. C. 2011. "Global remote sensing survey validation of canadian land cover and land use classifications". Vancouver, Canada. University of British Columbia.

Belgiu, M., and Drăgu, L. 2016. "Random forest in remote sensing: A review of applications and future directions." *ISPRS Journal of Photogrammetry and Remote Sensing*, Vol. 114: pp. 24–31. doi:10.1016/j.isprsjprs.2016.01.011.

Bergeron, Y., Chen, H. Y. H., Kenkel, N. C., Leduc, A. L., and Macdonald, S. E. 2014. "Boreal mixedwood stand dynamics: Ecological processes underlying multiple pathways." *Forestry Chronicle*, Vol. 90(No. 2): pp. 202–213. doi:10.5558/tfc2014-039.

Bergeron, Y., and Harvey, B. 1997. "Basing silviculture on natural ecosystem dynamics: an approach applied to the southern boreal mixedwood forest of Quebec." *Forest*

Ecology and Management, Vol. 92(No. 1): pp. 235–242. doi:10.1016/S0378-1127(96)03924-2.

Bossard, M., Feranec, J., and Otahel, J. 2000. "CORINE Land Cover." *Technical Guide*. Copenhagen, Denmark: Official Publications of the European Communities.

Braaten, J. D., Cohen, W. B., and Yang, Z. 2015. "Automated cloud and cloud shadow identification in Landsat MSS imagery for temperate ecosystems." *Remote Sensing of Environment*, Vol. 169: pp. 128–138. doi:10.1016/j.rse.2015.08.006.

Breiman, L. 2001. "Random forests." *Machine Learning*, Vol. 45(No. 1): pp. 5–32. doi:10.1023/A:1010933404324.

Brosofske, K. D., Froese, R. E., Falkowski, M. J., and Banskota, A. 2014. "A review of methods for mapping and prediction of inventory attributes for operational forest management." *Forest Science*, Vol. 60(No. 4): pp. 733–756. doi:10.5849/forsci.12-134.

Cai, S., Liu, D., Sulla-Menashe, D., and Friedl, M. A. 2014. "Enhancing MODIS land cover product with a spatial–temporal modeling algorithm." *Remote Sensing of Environment*, Vol. 147: pp. 243–255. doi:10.1016/j.rse.2014.03.012.

Clark, M. L., Aide, T. M., Grau, H. R., and Riner, G. 2010. "A scalable approach to mapping annual land cover at 250 m using MODIS time series data: A case study in the Dry Chaco ecoregion of South America." *Remote Sensing of Environment*, Vol. 114(No. 11): pp. 2816–2832. doi:10.1016/j.rse.2010.07.001.

Cochran, W. G. 1977. *Sampling Techniques*. New York: John Wiley and Sons.

Comber, A., Fisher, P., and Wadsworth, R. 2005. "What is land cover?" *Environment and Planning B: Planning and Design*, Vol. 32(No. 2): pp. 199–209. doi:10.1068/b31135.

Coppin, P., Jonckheere, I., Nackaerts, K., Muys, B., and Lambin, E. 2004. "Digital change detection methods in ecosystem monitoring: a review." *International Journal of Remote Sensing*, Vol. 25(No. 9): pp. 1565–1596. doi:10.1080/0143116031000101675.

Crist, E. 1985. "A TM tasseled cap equivalent transformation for reflectance factor data." *Remote Sensing of Environment*, Vol. 306: pp. 301–306. doi:10.1016/0034-4257(85)90102-6.

Czaplewski, R. L., and Patterson, P. L. 2003. "Classification accuracy for stratification with remotely sensed data." *Forest Science*, Vol. 49(No. 3): pp. 402–408.

Ecological Stratification Working Group. 1995. "A National Ecological Framework for Canada. https://doi.org/Cat. No. A42-65/1996E

EEA. 2002. "Corine land cover 2000." *Technical guidelines. Technical report*.

Feyisa, G. L., Meilby, H., Fensholt, R., and Proud, S. R. 2014. "Automated Water Extraction Index: A new technique for surface water mapping using Landsat imagery." *Remote Sensing of Environment*, Vol. 140: pp. 23–35. doi:10.1016/j.rse.2013.08.029.

Foody, G. M. 2002. "Status of land cover classification accuracy assessment." *Remote Sensing of Environment*, Vol. 80: pp. 185–201. doi:10.1016/S0034-4257(01)00295-4.

Franklin, J. 1995. "Predictive vegetation mapping: geographic modelling of biospatial patterns in relation to environmental gradients." *Progress in Physical Geography*, Vol. 19(No. 4): pp. 474–499. doi:10.1177/030913339501900403.

Franklin, S. E., Ahmed, O. S., Wulder, M. A., White, J. C., Hermosilla, T., and Coops, N. C. 2015. "Large area mapping of annual land cover dynamics using multi-temporal change detection and classification of Landsat time series data." *Canadian Journal of Remote Sensing*, Vol. 41: pp. 293–314. doi:10.1080/07038992.2015.1089401.

Frolking, S., Palace, M. W., Clark, D. B., Chambers, J. Q., Shugart, H. H., and Hurtt, G. C. 2009. "Forest disturbance and recovery: A general review in the context of spaceborne remote sensing of impacts on aboveground biomass and canopy structure." *Journal of Geophysical Research: Biogeosciences*, Vol. 114: pp. G00E02. doi:10.1029/2008JG000911.

Fuller, R., Smith, G., and Devereux, B. 2003. "The characterisation and measurement of land cover change through remote sensing: problems in operational applications?" *International Journal of Applied Earth*, Vol. 4(No. 3): pp. 243–253. doi:10.1016/S0303-2434(03)00004-7.

Gader, P. D., Mystkowski, M., and Zhao, Y. Z. Y. 2001. "Landmine detection with ground penetrating radar using hidden Markov models." *IEEE Transactions on Geoscience and Remote Sensing*, Vol. 39(No. 6): pp. 1231–1244. doi:10.1109/36.927446.

Gómez, C., White, J. C., and Wulder, M. A. 2016. "Optical remotely sensed time series data for land cover classification: A review." *ISPRS Journal of Photogrammetry and Remote Sensing*, Vol. 116(No. 2016): pp. 55–72. doi:10.1016/j.isprsjprs.2016.03.008.

Griffiths, P., Linden, S. Van Der, Kuemmerle, T., and Hostert, P. 2013. "A pixel-based landsat compositing algorithm for large area land cover mapping." *IEEE Journal of Selected Topics in Applied Earth Observations and Remote Sensing*, Vol. 6(No. 5): pp. 2088–2101. doi:10.1109/JSTARS.2012.2228167.

Hansen, M. C., and Loveland, T. R. 2012. "A review of large area monitoring of land cover change using Landsat data." *Remote Sensing of Environment*, Vol. 122: pp. 66–74. doi:10.1016/j.rse.2011.08.024.

Henderson-Sellers, A., and Pitman, A. 1992. "Land-surface schemes for future climate models: Specification, aggregation, and heterogeneity." *Journal of Geophysical Research*, Vol. 97(No. 91): pp. 2687–2696. doi:10.1029/91JD01697.

Hermosilla, T., Wulder, M. A., White, J. C., Coops, N. C., and Hobart, G. W. 2015a. "An integrated Landsat time series protocol for change detection and generation of annual gap-free surface reflectance composites." *Remote Sensing of Environment*, Vol. 158: pp. 220–234. doi:10.1016/j.rse.2014.11.005.

Hermosilla, T., Wulder, M. A., White, J. C., Coops, N. C., and Hobart, G. W. 2015b. "Regional detection, characterization, and attribution of annual forest change from 1984 to 2012 using Landsat-derived time-series metrics." *Remote Sensing of Environment*, Vol. 170: pp. 121–132. doi:10.1016/j.rse.2015.09.004.

Hermosilla, T., Wulder, M. A., White, J. C., Coops, N. C., and Hobart, G. W. 2017. "Updating Landsat time series of surface-reflectance composites and forest change products with new observations." *International Journal of Applied Earth Observation and Geoinformation*, Vol. 63: pp. 104–111. doi:10.1016/j.jag.2017.07.013.

Hermosilla, T., Wulder, M. A., White, J. C., Coops, N. C., Hobart, G. W., and Campbell, L. B. 2016. "Mass

data processing of time series Landsat imagery: pixels to data products for forest monitoring." *International Journal of Digital Earth*, Vol. 9(No. 11): pp. 1035–1054. doi:10.1080/17538947.2016.1187673.

Homer, C., Huang, C., Yang, L., Wylie, B., and Coan, M. 2004. "Development of a2001 National Land-Cover Database for the United States." *Photogrammetric Engineering & Remote Sensing*, Vol. 70(No. 7): pp. 829–840. doi:10.14358/PERS.70.7.829.

Huang, C., Goward, S. N., Masek, J. G., Thomas, N., Zhu, Z., and Vogelmann, J. E. 2010. "An automated approach for reconstructing recent forest disturbance history using dense Landsat time series stacks." *Remote Sensing of Environment*, Vol. 114(No. 1): pp. 183–198. doi:10.1016/j.rse.2009.08.017.

Inglada, J., Vincent, A., Arias, M., Tardy, B., Morin, D., and Rodes, I. 2017. "Operational high resolution land cover map production at the country scale using satellite image time series." *Remote Sensing*, Vol. 9(No. 1): pp. 95. doi:10.3390/rs9010095.

Jarron, L. R., Hermosilla, T., Coops, N. C., Wulder, M. A., White, J. C., Hobart, G. W., and Leckie, D. G. 2017. "Differentiation of alternate harvesting practices using annual time series of landsat data." *Forests*, Vol. 8(No. 1): pp. 15

Johnstone, J. F., Hollingsworth, T. N., Chapin, F. S., and Mack, M. C. 2010. "Changes in fire regime break the legacy lock on successional trajectories in Alaskan boreal forest." *Global Change Biology*, Vol. 16(No. 4): pp. 1281–1295. doi:10.1111/j.1365-2486.2009.02051.x.

Kennedy, R. E., Yang, Z., and Cohen, W. B. 2010. "Detecting trends in forest disturbance and recovery using yearly Landsat time series: 1. LandTrendr — Temporal segmentation algorithms." *Remote Sensing of Environment*, Vol. 114: pp. 2897–2910. doi:10.1016/j.rse.2010.07.008.

Key, C. H., and Benson, N. C. 2006. "Landscape assessment (LA): Sampling and analysis methods." *USDA Forest Service Gen. Tech. Rep. RMRS-GTR-164-CD*.

Khatami, R., Mountrakis, G., and Stehman, S. V. 2017. "Mapping per-pixel predicted accuracy of classified remote sensing images." *Remote Sensing of Environment*, Vol. 191: pp. 156–167. doi:10.1016/j.rse.2017.01.025.

Lawrence, R. L., Wood, S. D., and Sheley, R. L. 2006. "Mapping invasive plants using hyperspectral imagery and Breiman Cutler classifications (randomForest)." *Remote Sensing of Environment*, Vol. 100(No. 3): pp. 356–362. doi:10.1016/j.rse.2005.10.014.

Lee, H. K., Lee, J., Kim, H., Ha, J. Y., and Lee, K. J. 2013. "Snoring detection using a piezo snoring sensor based on hidden Markov models." *Physiol. Meas*, Vol. 34: pp. 41–49. doi:10.1088/0967-3334/34/5/N41.

Liu, D., and Cai, S. 2012. "A spatial-temporal modeling approach to reconstructing land-cover change trajectories from multi-temporal satellite imagery." *Annals of the Association of American Geographers*, Vol. 102(No. 6): pp. 1329–1347. doi:10.1080/00045608.2011.596357.

Liu, H., and Zhou, Q. 2004. "Accuracy analysis of remote sensing change detection by rule-based rationality evaluation with post-classification comparison." *International Journal of Remote Sensing*, Vol. 25(No. 5): pp. 1037–1050. doi:10.1080/0143116031000150004.

Masek, J. G., Vermote, E. F., Saleous, N. E., Wolfe, R., Hall, F. G., Huemmrich, K. F., and Lim, T. K. 2006. "A Landsat surface reflectance dataset for North America, 1990–2000." *Geoscience and Remote Sensing Letters, IEEE*, Vol. 3(No. 1): pp. 68–72. doi:10.1109/LGRS.2005.857030.

Meyer, W. B., and Turner, B. L. 1992. "Human population growth and global land-use." *Annual Review of Ecology and Systematics*, Vol. 23: pp. 39–61. doi:10.1146/annurev.es.23.110192.000351.

Mitchell, S. W., Remmel, T. K., Csillag, F., and Wulder, M. A. 2008. "Distance to second cluster as a measure of classification confidence." *Remote Sensing of Environment*, Vol. 112: pp. 2615–2626. doi:10.1016/j.rse.2007.12.006.

National Resources Canada. 2016. *The State of Canada's Forests: Annual Report 2016*.

Oliver, C. D. 1981. "Forest development in North America following major disturbances." *Forest Ecology and Management*, Vol. 3(No. 3): pp. 153–168.

Olofsson, P., Foody, G. M., Herold, M., Stehman, S. V., Woodcock, C. E., and Wulder, M. A. 2014. "Good practices for estimating area and assessing accuracy of land change." *Remote Sensing of Environment*, Vol. 148: pp. 42–57. doi:10.1016/j.rse.2014.02.015.

Olthof, I., Butson, C., and Fraser, R. 2005. "Signature extension through space for northern landcover classification: A comparison of radiometric correction methods." *Remote Sensing of Environment*, Vol. 95(No. 3): pp. 290–302. doi:10.1016/j.rse.2004.12.015.

Pakzad, K. 2002. "Knowledge based multitemporal interpretation." *International Archives of Photogrammetry Remote Sensing and Spatial Information Sciences*, Vol. 34(No. 3A): pp. 234–239.

Pal, M. 2005. "Random forest classifier for remote sensing classification." *International Journal of Remote Sensing*, Vol. 26(No. 1): pp. 217–222. doi:10.1080/01431160412331269698.

Pelletier, C., Valero, S., Inglada, J., Champion, N., and Dedieu, G. 2016. "Assessing the robustness of Random Forests to map land cover with high resolution satellite image time series over large areas." *Remote Sensing of Environment*, Vol. 187: pp. 156–168. doi:10.1016/j.rse.2016.10.010.

Pelletier, C., Valero, S., Inglada, J., Champion, N., and Sicre, C. M. 2017. "Effect of training class label noise on classification performances for land cover mapping with satellite image time series." *Remote Sensing*, Vol. 9: pp. 173. doi:10.3390/rs9020173.

Pielke, R. A., Pitman, A., Niyogi, D., Mahmood, R., McAlpine, C., Hossain, F., and de Noblet, N. 2011. "Land use/land cover changes and climate: modeling analysis and observational evidence." *Wiley Interdisciplinary Reviews: Climate Change*, Vol. 2(No. 6): pp. 828–850.

Pouliot, D., Latifovic, R., Zabcic, N., Guindon, L., and Olthof, I. 2014. "Development and assessment of a 250 m spatial resolution MODIS annual land cover time series (2000–2011) for the forest region of Canada derived from change-based updating." *Remote Sensing of Environment*, Vol. 140: pp. 731–743. doi:10.1016/j.rse.2013.10.004.

Radke, R. J., Andra, S., Al-Kofahi, O., and Roysam, B. 2005. "Image change detection algorithms: a systematic survey." *IEEE Transactions on Image Processing: A Publication of the IEEE Signal Processing Society*, Vol. 14(No. 3): pp. 294–307. doi:10.1109/TIP.2004.838698.

Remmel, T. K., Csillag, F., Mitchell, S., and Wulder, M. A. 2005. "Integration of forest inventory and satellite imagery: A Canadian status assessment and research issues." *Forest Ecology and Management*, Vol. 207(No. 3): pp. 405–428. doi:10.1016/j.foreco.2004.11.023.

Roberts, D., and Cooper, S. 1989. "Concepts and techniques of vegetation mapping." In D. Fergusson, P. Morgan, and F. D. Johnsson (Eds.), *Land Classifications Based on Vegetation: Applications for Resource Management*. (pp. 90–96). Ogden, UT: USDA Forest Service.

Roy, D. P., Kovalskyy, V., Zhang, H., Yan, L., and Kommareddy, I. 2015. "The utility of landsat data for global long term terrestrial monitoring." In *Remote Sensing Time Series* Vol. 22: pp. 289–305.

Roy, D. P., Wulder, M. A., Loveland, T. R., Woodcock, C. E., Allen, R. G., Anderson, M. C., and Zhu, Z. 2014. "Landsat-8: Science and product vision for terrestrial global change research." *Remote Sensing of Environment*, Vol. 145: pp. 154–172. doi:10.1016/j.rse.2014.02.001.

Schmidt, G. L., Jenkerson, C. B., Masek, J., Vermote, E., and Gao, F. 2013. "Landsat ecosystem disturbance adaptive processing system (ledaps) algorithm description. Reston, VA: U.S. Geological Survey.

Schroeder, T. A., Schleeweis, K. G., Moisen, G. G., Toney, C., Cohen, W. B., Freeman, E. A., and Huang, C. 2017. "Testing a Landsat-based approach for mapping disturbance causality in U.S. forests." *Remote Sensing of Environment*, Vol. 195: pp. 230–243. doi:10.1016/j.rse.2017.03.033.

Seedre, M., Taylor, A. R., Brassard, B. W., Chen, H. Y. H., and Jõgiste, K. 2014. "Recovery of ecosystem carbon stocks in young boreal forests: A comparison of harvesting and wildfire disturbance." *Ecosystems*, Vol. 17: pp. 851–863. doi:10.1007/s10021-014-9763-7.

Skole, D., Justice, C., Townshend, J. R. G., and Janetos, A. C. 1997. "A land cover change monitoring program: Strategy for an international effort." *Mitigation and Adaptation Strategies for Global Change*, Vol. 2: pp. 157–175. doi:10.1007/BF02437201.

Song, C., Woodcock, C. E., Seto, K. C., Pax-Lenney, M., and Macomber, S. A. 2001. "Classification and change detection using Landsat TM data: when and how to correct atmospheric effects?" *Remote Sensing of Environment*, Vol. 75(No. 2): pp. 230–244. doi:10.1016/S0034-4257(00)00169-3.

Stehman, S. V., and Czaplewski, R. 2003. "Introduction to special issues on map accuracy." *Environmental and Ecological Statistic*, Vol. 10: pp. 301–308. doi:10.1023/A:1025138423071.

Strahler, A. H., Logan, T. L., and Bryant, N. A. 1978. "Improving forest cover classification accuracy from Landsat by incorporating topographic information." In *International Symposium on Remote Sensing of Environment* (pp. 16). Manila, Philippines.

Tachikawa, T., Kaku, M., Iwasaki, A., Gesch, D., Oimoen, M., Zhang, Z., and Carabajal, C. 2011. "ASTER Global Digital Elevation Model Version 2 – Summary of Validation Results. NASA.

Trier, Ø. D., and Salberg, A.B. 2011. "Time-series analysis of satellite images for forest cover change monitoring in Tanzania." In *1st EARSeL Workshop on Operational Remote Sensing in Forest Management* (pp. 1–12). Prague, Czech Republic.

Tucker, C. J. 1979. "Red and photographic infrared linear combinations for monitoring vegetation." *Remote Sensing of Environment*, Vol. 8: pp. 127–150. doi:10.1016/0034-4257(79)90013-0.

Verbesselt, J., Hyndman, R., Zeileis, A., Culvenor, D. S., and Newnham, G. J. 2010. "Detecting trend and seasonal changes in satellite image time series." *Remote Sensing of Environment*, Vol. 114(No. 1): pp. 106–115. doi:10.1016/j.rse.2009.08.014.

Vogelmann, J. E., Howard, S. M., Yang, L., Larson, C. R., Wylie, B. K., and Van Driel, N. 2001. "Completion of the 1990 s national land cover data set for the conterminous United States from Landsat Thematic Mapper data and ancillary data sources." *Photogrammetric Engineering and Remote Sensing*, Vol. 67(No. 6): pp. 650–662.

Wessels, K. J., Bergh, F. van den, Roy, D. P., Salmon, B. P., Steenkamp, K. C., MacAlister, B., and Jewitt, D. 2016. "Rapid land cover map updates using change detection and robust random forest classifiers." *Remote Sensing*, Vol. 8(No. 11): pp. 1–24.

White, J. C., and Wulder, M. A. 2014. "The Landsat observation record of Canada: 1972–2012." *Canadian Journal of Remote Sensing*, Vol. 39(No. 6): pp. 455–467. doi:10.5589/m13-053.

White, J. C., Wulder, M. A., Hermosilla, T., Coops, N. C., and Hobart, G. W. 2017. "Annual characterization of 25 years of forest disturbance and recovery in Canada with Landsat." *Remote Sensing of Environment*, Vol. 194: pp. 303–321. doi:10.1016/j.rse.2017.03.035.

White, J. C., Wulder, M. A., Hobart, G. W., Luther, J. E., Hermosilla, T., Griffiths, P., and Guindon, L. 2014. "Pixel-based image compositing for large-area dense time series applications and science." *Canadian Journal of Remote Sensing*, Vol. 40(No. 3): pp. 192–212. doi:10.1080/07038992.2014.945827.

Woodcock, C. E., Allen, R., Anderson, M., Belward, A., Bindschadler, R., Cohen, W., and Wynne, R. H. 2008. "Free Access to Landsat Imagery." *Science*, Vol. 320(No. 5879): pp. 1011. doi:10.1126/science.320.5879.1011a.

Woodcock, C. E., Macomber, S. A., Pax-Lenney, M., and Cohen, W. B. 2001. "Monitoring large areas for forest change using Landsat: Generalization across space, time and Landsat sensors." *Remote Sensing of Environment*, Vol. 78(No. 1): pp. 194–203. doi:10.1016/S0034-4257(01)00259-0.

Wulder, M. A., and Coops, N. C. 2014. "Make Earth observations open access." *Nature*, Vol. 513(No. 7516)(09/2014): pp. 30–31. doi:10.1038/513030a.

Wulder, M. A., Cranny, M., Dechka, J., and White, J. C. 2004. "An illustrated methodology for land cover mapping of forests with Landsat-7 ETM+ data: Methods in support of EOSD land cover, Version 3. Natural Resources Canada, Canadian Forest Service." *Pacific Forestry Centre, Victoria, BC, Canada*, Vol. 35(No. March): pp. 1–35.

Wulder, M. A., Franklin, S. E., White, J. C., Cranny, M. M., and Dechka, J. A. 2004. "Inclusion of topographic variables in an unsupervised classification of satellite imagery." *Canadian Journal of Remote Sensing*, Vol. 30(No. 2): pp. 137–149. doi:10.5589/m03-063.

Wulder, M. A., Hilker, T., White, J. C., Coops, N. C., Masek, J. G., Pflugmacher, D., and Crevier, Y. 2015. "Virtual constellations for global terrestrial monitoring." *Remote Sensing of Environment*, Vol. 170: pp. 62–76. doi:10.1016/j.rse.2015.09.001.

Wulder, M. A., Masek, J. G., Cohen, W. B., Loveland, T. R., and Woodcock, C. E. 2012. "Opening the archive: How free data has enabled the science and monitoring promise of Landsat." *Remote Sensing of Environment*, Vol. 122: pp. 2–10. doi:10.1016/j.rse.2012.01.010.

Wulder, M. A., White, J. C., Cranny, M. M., Hall, R. J., Luther, J. E., Beaudoin, A., and Dechka, J. A. 2008. "Monitoring Canada' s forests. Part 1: Completion of the EOSD land cover project." *Canadian Journal of Remote Sensing*, Vol. 34(No. 6): pp. 549–562. doi: 10.5589/m08-066.

Wulder, M. A., White, J. C., Loveland, T. R., Woodcock, C. E., Belward, A. S., Cohen, W. B., and Roy, D. P. 2016. "The global Landsat archive: Status, consolidation, and direction." *Remote Sensing of Environment*, Vol. 185: pp. 271–283. doi: 10.1016/j.rse.2015.11.032.

Wulder, M. A., White, J. C., Magnussen, S., and McDonald, S. 2007. "Validation of a large area land cover product using purpose-acquired airborne video." *Remote Sensing of Environment*, Vol. 106(No. 4): pp. 480–491. doi:10.1016/j.rse.2006.09.012.

Xian, G., Homer, C., and Fry, J. 2009. "Updating the 2001 National Land Cover Database land cover classification to 2006 by using Landsat imagery change detection methods." *Remote Sensing of Environment*, Vol. 113(No. 6): pp. 1133–1147. doi:10.1016/j.rse.2009.02.004.

Yu, S. Z. 2010. "Hidden semi-Markov models." *Artificial Intelligence*, Vol. 174: pp. 215–243. doi:10.1016/j.artint.2009.11.011.

Yu, S. Z., and Kobayashi, H. 2006. "Practical implementation of an efficient forward-backward algorithm for an explicit-duration hidden Markov model." *IEEE Transactions on Signal Processing*, Vol. 54(No. 5): pp. 1947–1951. doi:10.1109/TSP.2006.872540.

Zhang, H. K., and Roy, D. P. 2017. "Using the 500 m MODIS land cover product to derive a consistent continental scale 30 m Landsat land cover classification." *Remote Sensing of Environment*, Vol. 197: pp. 15–34. doi:10.1016/j.rse.2017.05.024.

Zhu, Z., Gallant, A. L., Woodcock, C. E., Pengra, B., Olofsson, P., Loveland, T. R., and Auch, R. F. 2016. "Optimizing selection of training and auxiliary data for operational land cover classification for the LCMAP initiative." *ISPRS Journal of Photogrammetry and Remote Sensing*, Vol. 122: pp. 206–221. doi:10.1016/j.isprsjprs.2016.11.004.

Zhu, Z., and Woodcock, C. E. 2012. "Object-based cloud and cloud shadow detection in Landsat imagery." *Remote Sensing of Environment*, Vol. 118: pp. 83–94. doi:10.1016/j.rse.2011.10.028.

Zhu, Z., and Woodcock, C. E. 2014. "Continuous change detection and classification of land cover using all available Landsat data." *Remote Sensing of Environment*, Vol. 144: pp. 152–171. doi:10.1016/j.rse.2014.01.011.